STM JOURNALS

Trends in
Machine Design

ISSN: 2455-3352
Volume 13, Issue 1, 2026
January–April
DOI (Journal): 10.37591/TMD

https://journals.stmjournals.com/tmd

Review TMD

Review on Severe Plastic Deformation Techniques for Bulk Materials: Deformation Behavior and Properties

Nagendra Singh[1,*], Gopal Sharma[2]

Abstract

This paper presents a detailed review of the efficient application of Severe Plastic Deformation for the fabrication of ultra-fine-grained and nanostructured crystalline bulk materials. Severe Plastic Deformation allows substantial grain refinement while largely preserving the original dimensions of the workpiece, making it especially suitable for ductile materials capable of sustaining very high strains under elevated hydrostatic pressure prior to failure. The study investigates the grain refinement mechanisms involved in Severe Plastic Deformation and their effects on metal microstructures, along with its use in difficult-to-deform brittle materials such as tungsten oxide, B_2O_3 glasses, and amorphous substances. It also outlines the advantages and limitations of various Severe Plastic Deformation techniques, their practical applications, and possible hybrid approaches. This review emphasizes recent advances in process development that may support the industrial adoption of certain Severe Plastic Deformation techniques. By filling this gap in the existing literature, the review demonstrates the potential of Severe Plastic Deformation in metal processing and in the creation of new ultra-fine-grained materials with improved mechanical properties. Equal Channel Angular Pressing (ECAP) is a potential technique for producing an ultra-fine-grained microstructure and improving material properties. Several parameters—such as the processing route, die angle, number of passes, and operating temperature—play a crucial role in determining the mechanical behavior and microstructural evolution of materials subjected to the ECAP process. Considerable attention has been given to the evolution of magnesium alloy microstructures and their mechanical properties after processing by the ECAP method. It has been observed that a finer microstructure with enhanced mechanical performance can be achieved by using lower processing temperatures, a higher number of passes, and a smaller die angle.

Keywords: SPD techniques, Metallic bulk samples, SPD characteristics, Industrial SPD approaches

***Author for Correspondence**
Nagendra Singh
E-mail: singh.mech2008@gmail.com

[1]Assistant Professor, Department of Mechanical Engineering, Institute of Engineering and Technology, Dr. Bhimrao Ambedkar University, Khandari Campus, Agra, Uttar Pradesh, India
[2]Research Scholar, Department of Mechanical Engineering, Eshan College of Engineering Near Raipura Jaat, Mathura, Uttar Pradesh, India

Received Date: February 12, 2026
Accepted Date: February 14, 2026
Published Date: February 25, 2026

Citation: Nagendra Singh, Gopal Sharma. Review on Severe Plastic Deformation Techniques for Bulk Materials: Deformation Behavior and Properties. Trends in Machine Design. 2026; 13(1): 40–72p.

INTRODUCTION

The advancement of materials with improved mechanical properties is a crucial area of research in materials science. Severe Plastic Deformation has proven to be a promising method for fabricating ultrafine-grained materials with outstanding performance characteristics. This review examines the effective use of Severe Plastic Deformation in the production of ultra-fine-grained and nanostructured crystalline materials, emphasizing the different techniques applied to bulk materials. Severe Plastic Deformation techniques are widely applied in various industries such as aerospace, biomedical implants, automotive, electronics, energy, and sports equipment. In the aerospace sector, Severe Plastic Deformation is used to produce ultrafine-grained

titanium, aluminum, and magnesium alloys with enhanced strength and fatigue resistance [1-20]. Among the methods developed for grain refinement, Severe Plastic Deformation techniques are especially significant and form the main focus of this review. These techniques are widely favored because they can achieve substantial grain refinement in fully dense, bulk-scale workpieces, making them highly promising for structural applications [21-40].

The grain sizes that can be achieved range from the submicrometer scale (100–1000 nm) to the nanometer scale (<100 nm). Materials processed through Severe Plastic Deformation with these grain sizes are typically described as nanoSPD materials; however, only those with grain sizes below 100 nm are classified as nanostructured by the standard definition. Several detailed review articles have addressed different nanoSPD processing techniques [2]. For specific information, readers are directed to the original studies, while this paper provides only a brief overview of the general SPD methodology, emphasizing the shared characteristics and key distinctions among nanoSPD processes [41-60]. The presented summary does not claim to cover all existing manufacturing approaches. In biomedical implant applications, Severe Plastic Deformation is used to produce materials with superior mechanical performance and biocompatibility, including ultrafine-grained titanium alloys that exhibit improved strength and biological compatibility. In the automotive sector, Severe Plastic Deformation is employed to produce ultrafine-grained aluminum, magnesium, and steel alloys with enhanced strength and ductility. Similarly, the electronics industry applies Severe Plastic Deformation to develop materials exhibiting high thermal and electrical conductivity [61-80].

Table 1. Diagrammatic representation of selected conventional and advanced Severe Plastic Deformation techniques.

S.N.	Basic Processes	Schematic illustration	Equivalent Strain	Ref.
1.	Equal channel angular pressing (ECAP)	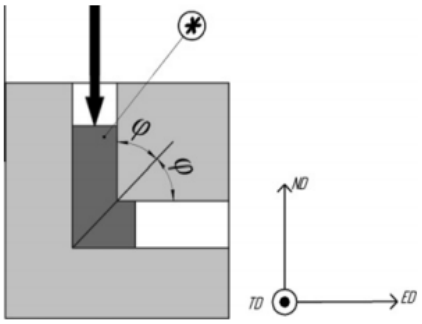	$\varepsilon_{eff} = N\frac{2}{\sqrt{3}}cot(\phi)$ N, the number of ECAP passes	[39]
2.	Accumulative roll bonding (ARB)	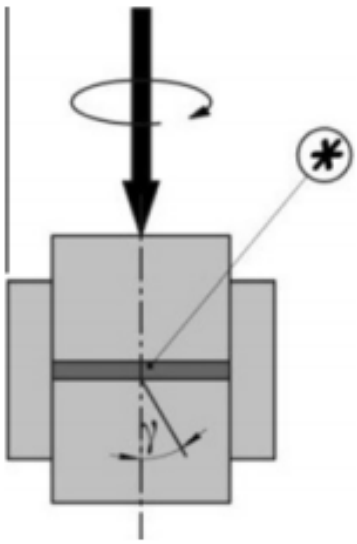	$\varepsilon_{eff} = N\frac{2}{\sqrt{3}}\frac{\pi r}{t}$ r, the distance from the axis, t, the thickness of the sample, N, the number of revolutions	[34]

3.	Accumulative roll bonding (ARB)	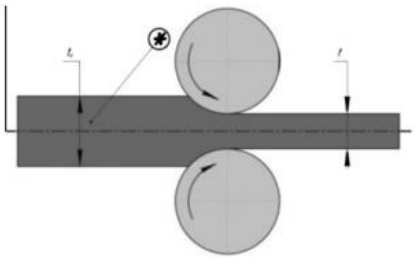	$\varepsilon_{eff} = N\frac{2}{\sqrt{3}}\ln\left(\frac{t_0}{t}\right)$ t_0, the initial thickness of the sample, t , the thickness of the sample after rolling, N , the number of passes	[54]
4.	Multi-axial forging	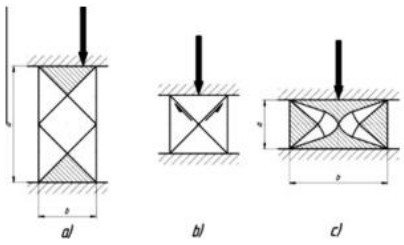	$\varepsilon_{eff} = N\frac{2}{\sqrt{3}}\ln\left(\frac{a}{b}\right)$ Strain is non-uniform, N, the number of processing steps	[57]
5.	Twist extrusion (TE)	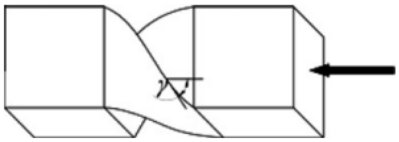	$\varepsilon_{eff}^{min} \approx 0.4+0.1\tan\gamma$ $\varepsilon_{eff}^{min} \approx N\frac{2}{\sqrt{3}}\tan\gamma$ γ is the twist line slope; N is the number of passes. Deformation is non-uniform	[61]
6.	Repetitive side extrusion	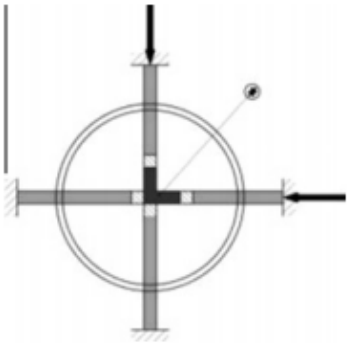	ECAP	[65]
7.	Rotary-die ECAP	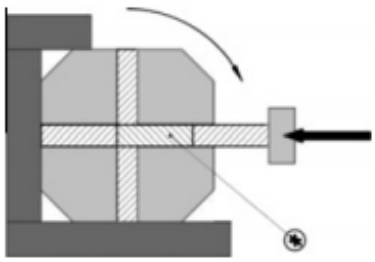	ECAP equivalent	[66]
8.	Cyclic extrusion-compression (CEC)	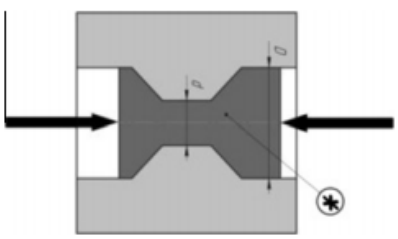	$\varepsilon_{eff} = N\,4ln\left(\frac{D}{d}\right)$ N, number of cycles	[75]

9.	Cyclic close-die forging (CCDF)	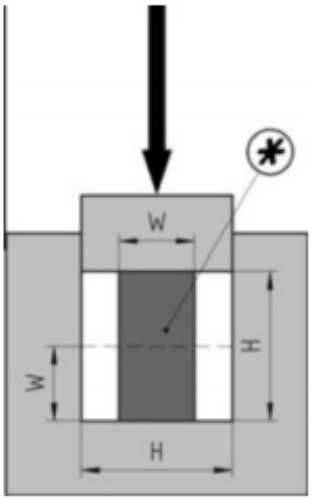	$\varepsilon_{eff}=N\ \frac{2}{\sqrt{3}} ln\left(\frac{H}{W}\right)$ N, number of cycles	[76]
10.	Repetitive corrugation and straightening (RCS)	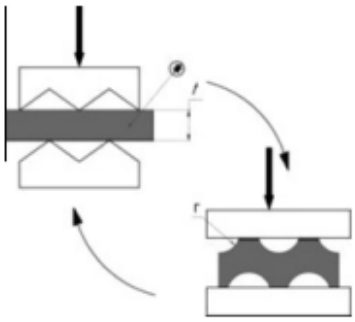	$\varepsilon_{eff}=N\ \frac{4}{\sqrt{3}} ln\left(\frac{r+t}{r+0.5t}\right)$ N, number of cycles	[72]
11.	Integrated extrusion+ECAP	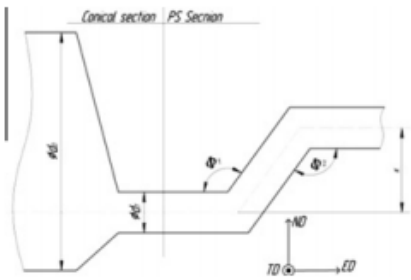	Integrated extrusion + ECAP is process of Combines extrusion + ECAP in one tool, enabling continuous production of bulk UFG materials with improved strength, ductility, and properties.	[10,11]
12.	Parallel channel ECAP (PC-ECAP)	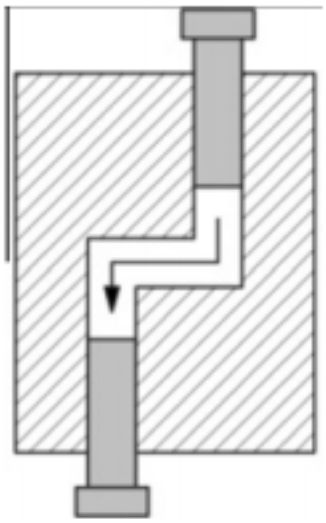	ECAP equivalent	[67]

13.	ECAP-Conform	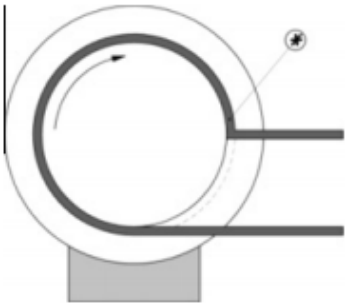	ECAP-Conform combines ECAP + Conform process to produce UFG metals continuously, strengthening Al and Cu alloys for wires, implants, etc.	[37, 20]
14.	Con-shearing	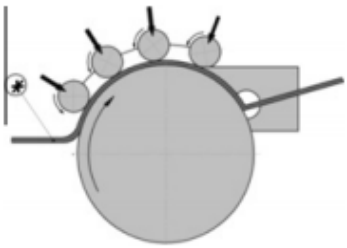	Con-shearing is a continuous shear deformation process that improves metal properties (like deep drawability) in coiled strips, or refers to high-speed metal cutting in rolling mills, or advanced CNC shearing machines for precise cuts.	[21]
15.	Continous confined strip shearing (C2S2)	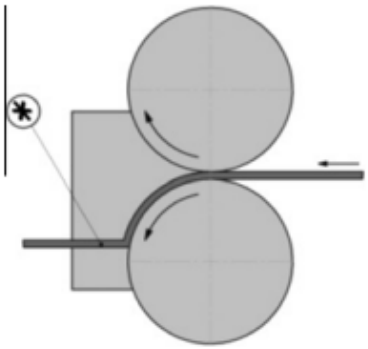	C2S2 is a SPD technique that refines grain structure and boosts properties in sheet materials through continuous shearing and deformation.	[22]
16.	Continuous repetitive corrugating and straightening (RCS)	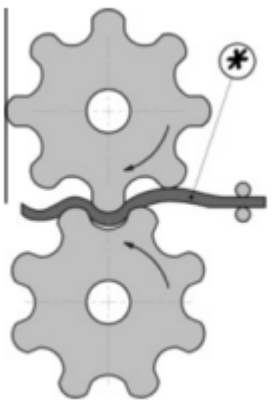	Continuous RCS is a simple yet effective way to process sheet materials and enhance their properties.	[73]
17.	Incremental ECAP (I-ECAP)	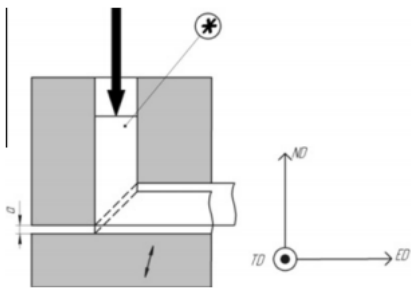	I-ECAP: Incremental ECAP technique for continuous processing of bars, plates, and sheets, producing ultrafine-grained materials with improved strength, ductility, and reduced anisotropy.	[26]

18.	Continuous High pressure torsion	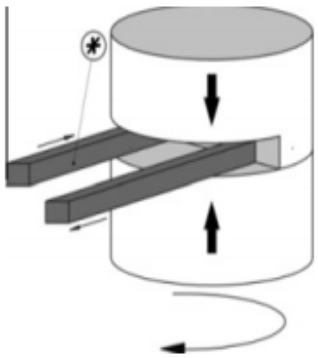	Refines grain structure in metals, Applies high pressure and shear strain, Consistent results with other CHPT methods, Can be used for continuous processing	[27]
19.	Continuous manufacturing of bolts	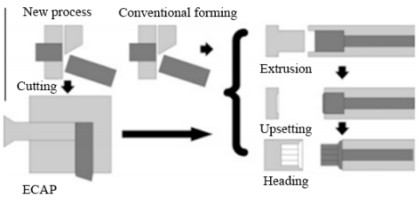	A continuous manufacturing system to apply an ECAP to bolt forming was developed. A spring-loaded auto-fastening system with split-dies for the ECAP was devised. The UTS of the microstructure-refined bolt was 6.2% higher than the conventional one.	[29]
20.	CGP-Constrained groove pressing	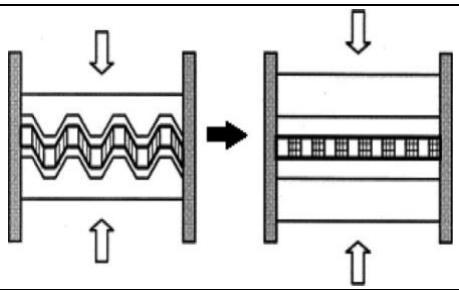	Strengthens sheet metals via SPD, Induces shear strain with grooved + flat dies, Refines grains to ultrafine levels (sub-micron/nano), No change in material dimensions, Enhances strength, hardness, and properties.	[14]

Severe Plastic Deformation methods enable the production of ultrafine-grained copper, aluminum, and nickel alloys with improved thermal and electrical conductivity. In the energy industry, these techniques are used to fabricate ultrafine-grained stainless steels, nickel-based alloys, and titanium alloys that exhibit enhanced strength and corrosion resistance.

The sports equipment sector gains from ultrafine-grained aluminum and titanium alloys produced through Severe Plastic Deformation, as these materials provide enhanced strength and fatigue resistance, making them well suited for lightweight, high-performance applications.

Overall, Severe Plastic Deformation techniques are applied across a wide range of industries, and further development of these methods can result in materials with superior properties [2]. Severe Plastic Deformation (SPD) is widely recognized as the most effective approach for producing bulk ultrafine-grained and nanostructured materials with outstanding performance.

Various Severe Plastic Deformation methods have been developed for processing sheet materials and bulk solids. Over the past decade, significant efforts have also been directed toward developing efficient SPD techniques for the fabrication of cylindrical tubes.

This paper reviews Severe Plastic Deformation processes designed to produce ultrafine-grained and nanostructured tubes and examines their influence on material properties. The study first introduces the various tube-based SPD processes and then compares them in terms of their advantages and limitations, considering both processing aspects and resulting material properties [71].

SEVERE PLASTIC DEFORMATION MECHANISMS

Severe Plastic Deformation Techniques for Bulk Samples

High Pressure Torsion (HPT)

The HPT method, introduced in and illustrated in Figure 1, is an effective Severe Plastic Deformation technique that applies a high shear strain to the specimen. The associated strain is calculated using Eq. (1). This method offers several advantages; unlike many Severe Plastic Deformation techniques that impose cyclic strain, HPT provides a continuous variation of strain [3]. In the HPT process, large shear strains can be achieved relatively easily. Owing to the high hydrostatic pressure involved—something that is difficult to attain with other Severe Plastic Deformation techniques—HPT is capable of processing hard-to-deform materials. Furthermore, reversing the rotation direction induces Severe Plastic Deformation, a feature that is also observed in several other Severe Plastic Deformation methods [4]. The strain is calculated using Eq. (1):

$$\varepsilon_{eff} = N\frac{2}{\sqrt{3}}\frac{\pi r}{t} \tag{1}$$

Where r represents the distance from the center, t denotes the thickness of the material, and N indicates the number of revolutions.

However, this technique is limited to processing small, coin-shaped specimens, which restricts its application primarily to research due to size constraints. In addition, it may produce non-uniform deformation, which can be mitigated by carefully controlling the thickness-to-diameter ratio of the sample. This ratio depends on the material and should not exceed a certain limit [5]. Figure 2(a)–(c) presents the evolution of grain structure along the radial direction in HPT-processed samples. Three locations—edge, middle, and center—are selected to illustrate the variation in grain size, demonstrating the inverse relationship between grain size and strain within the material, as previously reported in the literature [6,7].

HPT provides multiple benefits, such as continuous variation of strain, straightforward application of shear strain, and the ability to process hard-to-deform materials owing to the high hydrostatic pressure involved. Additionally, reversing the direction of rotation can induce Severe Plastic Deformation. However, HPT has certain drawbacks, including its restriction to small, coin-shaped specimens, which makes it primarily appropriate for research applications. Another challenge is non-uniform

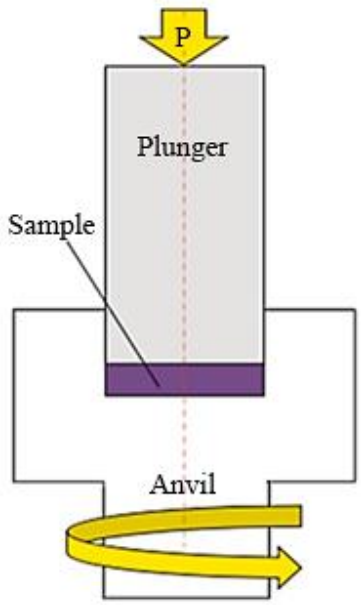

Figure 1. Presents a schematic diagram of the High Pressure Torsion (HPT) process [3].

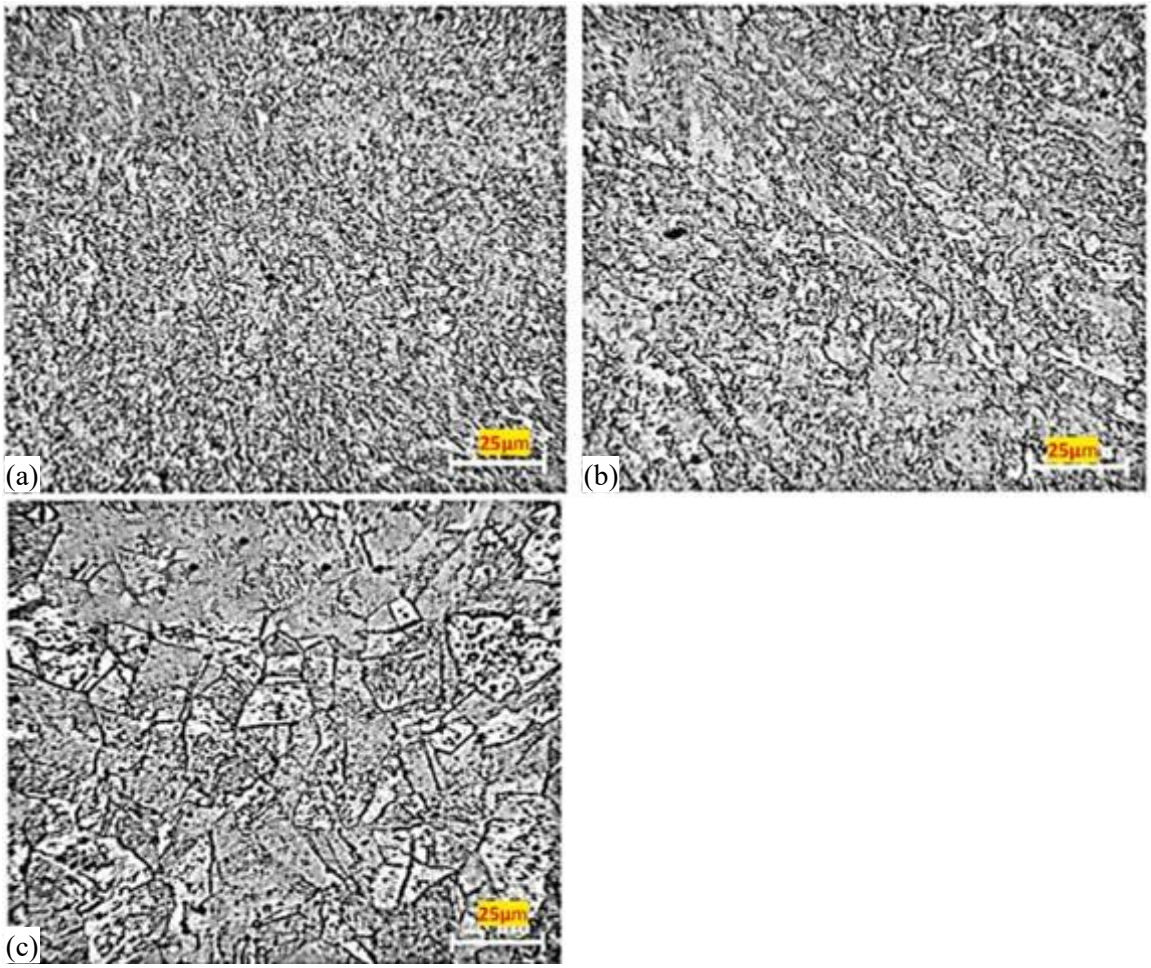

Figure 2. Displays optical micrographs depicting the grain size of an HPT-processed specimen [7]. (a) Edge, (b) middle, and (c) center

deformation, which can be reduced by optimizing the thickness-to-diameter ratio of the sample. Figure 2(a)–(c) illustrates the evolution of grain structure in HPT-processed samples, showing that grain size decreases with increasing strain, as reported in earlier studies [6,7].

High Pressure Torsion Extrusion (HPTE)

The HPTE technique is a recently developed Severe Plastic Deformation method for metals and alloys, designed to produce long ultrafine-grained products with high dislocation density by imposing intense shear deformation within the active zone, thereby overcoming earlier size limitations [72-75]. The method consists of extruding a cylindrical sample through coaxial rotating containers, where shear deformation takes place at the contact interface, as illustrated schematically in Figure 3 [8]. Copper specimens were processed using the HPTE technique through both experimental and analytical approaches. Figure 4(a) presents TEM bright-field (BF) images showing that no precipitates were detected within the grains after HPTE processing [9]. The grain morphology appears equiaxed, as illustrated in Figure 4(b), and the average grain size is smaller compared to that in the middle region. SEM-BSE images further indicate that the volume fraction of second-phase particles is lower than that observed in the core area [76-82].

Equal-channel Angular Pressing (ECAP)

ECAP, or Equal-Channel Angular Extrusion, is illustrated schematically in Figure 5 for the conventional process. The die is composed of two channels of equal cross-section intersecting at a specific angle ϕ. Although this angle is commonly set at 90°, alternative angles such as 60° or 120° are

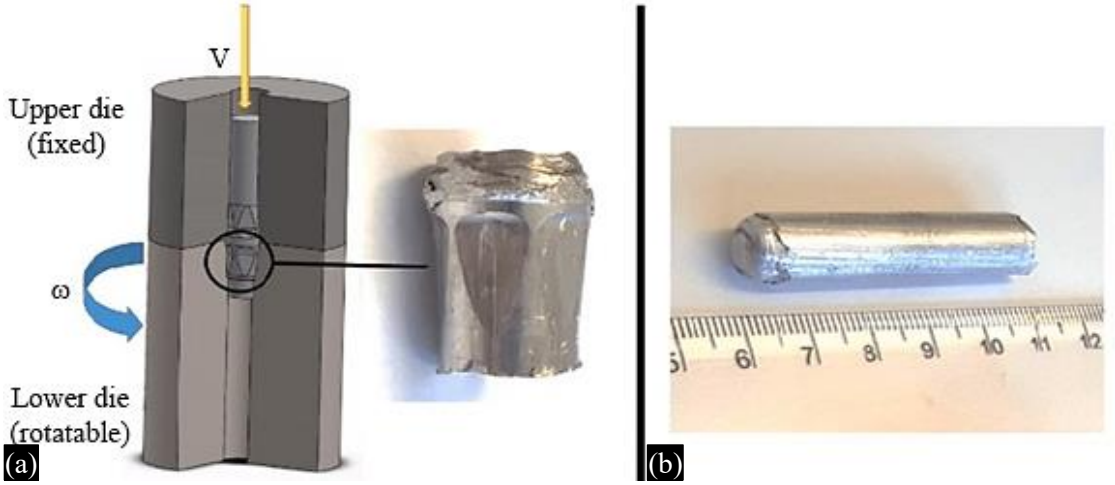

Figure 3. Presents a schematic representation of the HPTE method with a specimen being processed [10].

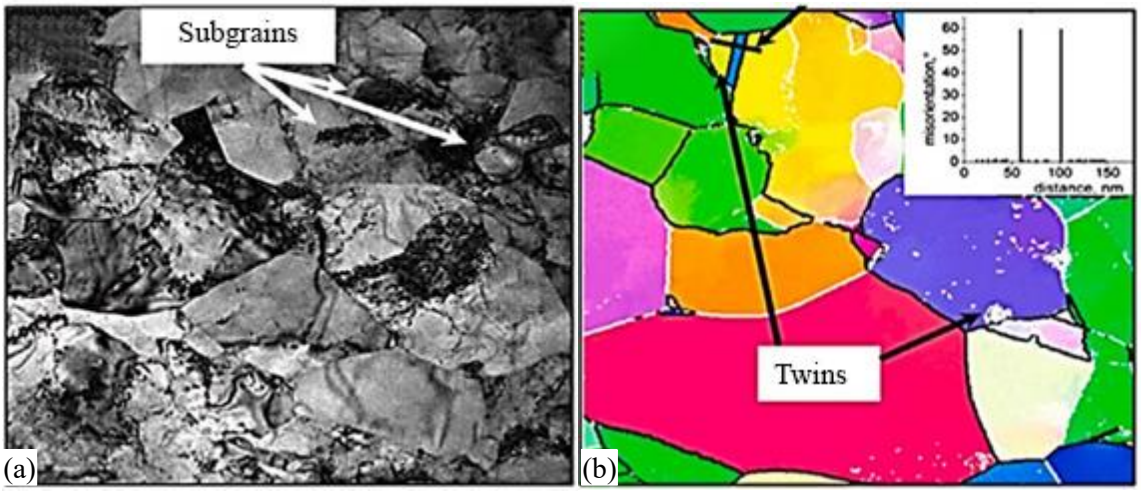

Figure 4. Displays the microstructure of copper processed by HPTE in the central region of the longitudinal section [9].

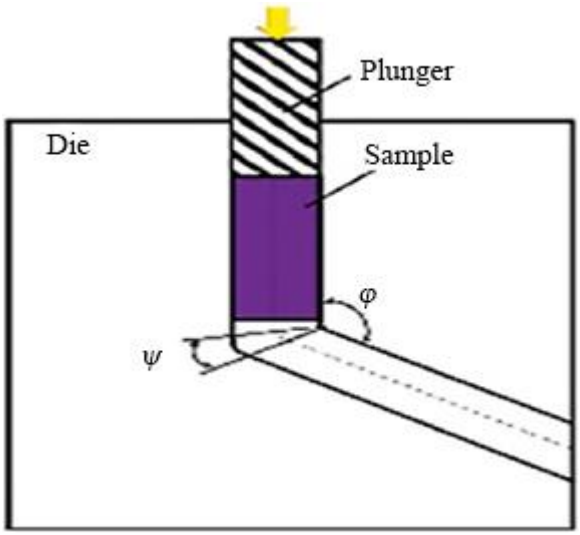

Figure 5. Presents a schematic illustration of the ECAP process used for processing bulk specimens [11].

Table 2. Presents various studies conducted on materials processed using the ECAP method.

Researcher	Topic	Objectives
Kim et al. [36]	Effect of channel angular pressing routes on the high strain rate deformation behavior of ultrafine-grained Mg alloys.	To study the fracture behavior and high strain rate (HSR) deformation of ultrafine-grained aluminum alloy after 1-pass (1P) and 8-pass (8P) ECAP processed through different routes. Additionally, to evaluate the effects on tensile and torsional properties, as well as the potential formation of adiabatic shear bands.
Suh et al. [37]	AZ31 alloy sheets processed through ECAP exhibit enhanced cold formability.	To examine the mechanical properties and the evolution of the microstructure, and to compare the results with the cold forming behavior.
Torre et al. [38]	Microstructure and properties of copper following 1–16 passes of equal channel angular extrusion.	To analyze the microstructure from 0 to 16 passes using TEM and XRD techniques, and to investigate the mechanical properties of the material after processing.
Eddahbi et al. [39]	Mechanical properties and texture of ECAP-processed EUROFER 97 steel.	To examine whether warm ECAP can assist in tempering EUROFER 97 to stabilize its grain structure and thereby enhance its mechanical performance within the service temperature range.

Table 3. Features of the Equal Channel Angular Pressing technique.

Attributes	Characteristics
Grain	Precision
The primary priority of the ECAP	The purpose of the operation is to enhance the strength of the material's crystalline structure. Continuous shearing and deformation as the specimen passes through the channel lead to a marked reduction in grain size and an increase in the number of grain boundaries. Consequently, the mechanical properties are enhanced, including strength, rigidity, and toughness.
Low Strain Rate	The Multi - pass process generally runs at low strain rates, that either decreases the probability of material flaws and cracks. The material can deform evenly without creating localised deformation zones thanks to the low strain rates, which also leads to a homogeneous microstructure.
High Strain	The ECAP process is capable of imposing a high level of strain, typically exceeding 4. Such large strains are necessary to introduce intense plastic deformation and promote effective grain refinement.

also employed. To facilitate insertion into the inlet channel, the specimen is machined slightly smaller than the channel dimensions. It is then forced into the deformation zone using a plunger, subjecting the sample to a substantial shear plastic strain [11]. The total strain after ϕ passes can be calculated using Eq. (2).

$$\varepsilon = \frac{2N}{\sqrt{3}} cot\left(\frac{\Phi}{2}\right) \tag{2}$$

Figure 6 illustrates the grain refinement mechanism in a pure titanium sample after a single ECAP pass. Micro-twin bands, characterized by dislocation walls and indicated by red arrows, are observed, leading to the formation of a lamellar structure.

This mechanism is likewise observed in face-centered cubic metals, such as copper, when subjected to high strain-rate processes including shock loading, ball milling, and dynamic plastic deformation. In these materials, the availability of active slip systems increases the dislocation density, promoting dislocation multiplication and movement, which in turn refines the microstructure [12].

Conversely, the twinning mechanism plays an important role in the plastic deformation of body-centered cubic and hexagonal close-packed metals, as well as brittle materials such as tungsten oxide and B_2O_3 glasses, since these materials possess limited slip systems at room temperature.

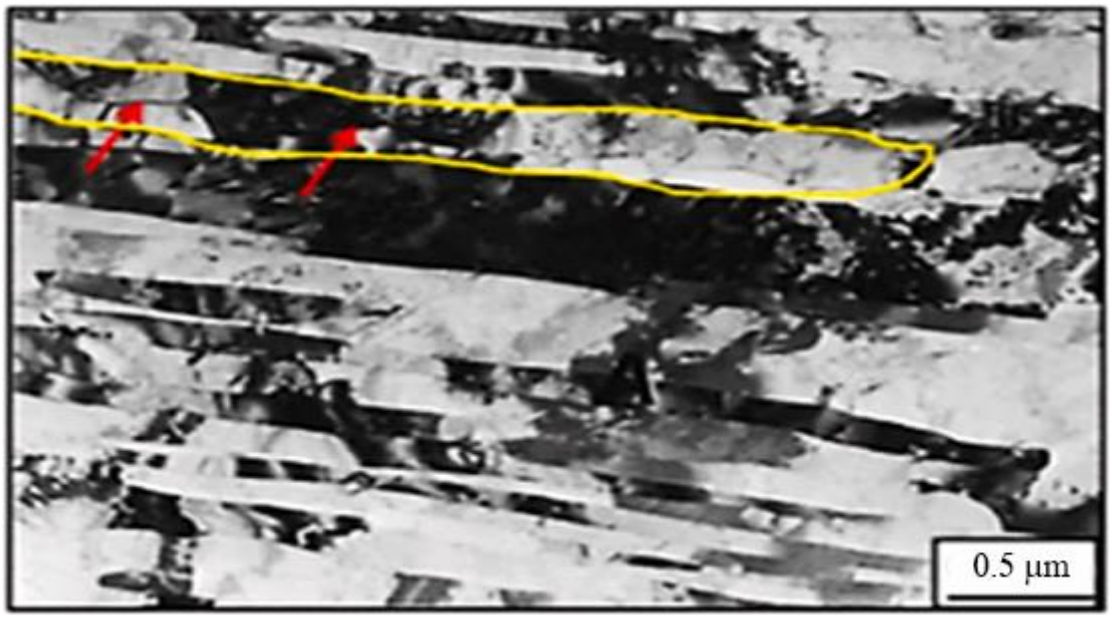

Figure 6. Displays a TEM image of a titanium sample processed by ECAP, emphasizing the presence of twinning and dislocation walls [13].

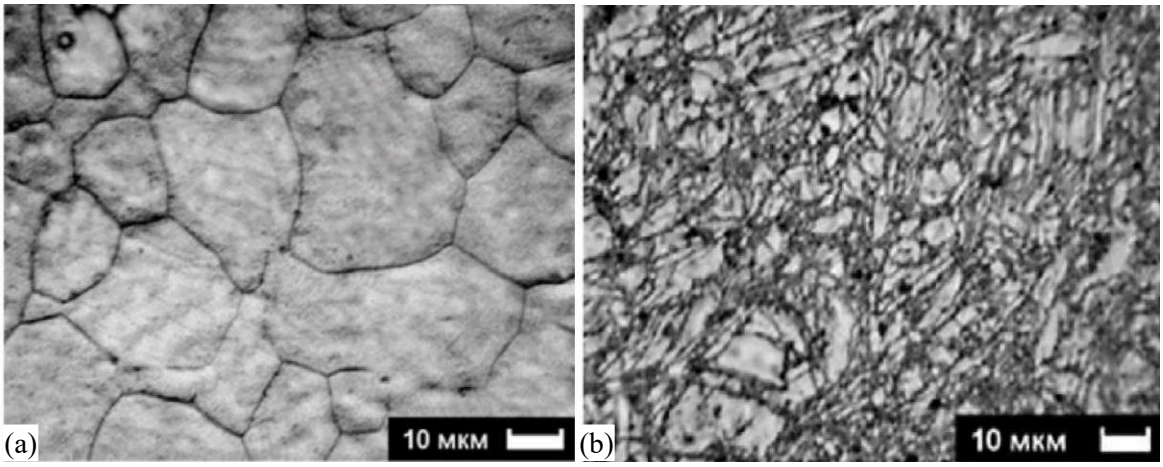

Figure 7. Displays the microstructure of AZ31 alloy (a) in the as-received condition and (b) after two passes at 200 °C [15].

This mechanism likewise influences ductile materials that are capable of enduring high hydrostatic pressures prior to failure. In addition, Severe Plastic Deformation brings about structural changes in these materials, resulting in enhanced mechanical properties [13,14].

The microstructural analysis indicates characteristic features of grain refinement. Figures 7(a) and (b) present SEM images of the AZ31 alloy before processing and after two ECAP passes at 200 °C. Initially, the grains exhibit an equiaxed morphology with typical triple junction features [83-.89] Following ECAP deformation, significant grain refinement occurs, accompanied by the formation of new high-angle grain boundaries and a large number of deformation twins [15].

Rotary-die (RD)

Figure 8 depicts the ECAP process employing rotating dies. In this method, a die containing two intersecting perpendicular channels is utilized. The specimen is introduced from the top of the die, as illustrated in Figure 8(a), and then driven sideways by a plunger. The operation is completed when the plunger reaches the flat surface, after which the entire die is rotated by 90°, as shown in Figure 8(b).

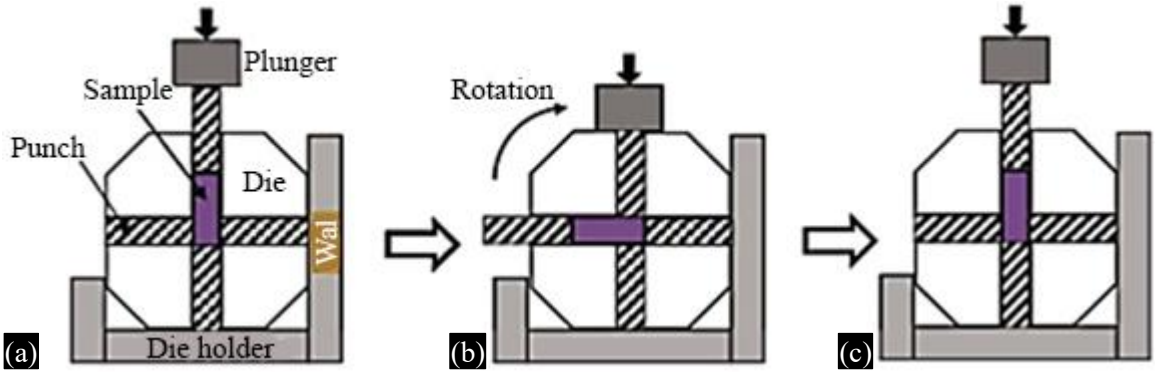

Figure 8. Depicts the rotary-die ECAP process: (a) initial state, (b) after a single pass, and (c) after a 90° rotation in preparation for the subsequent cycle [16].

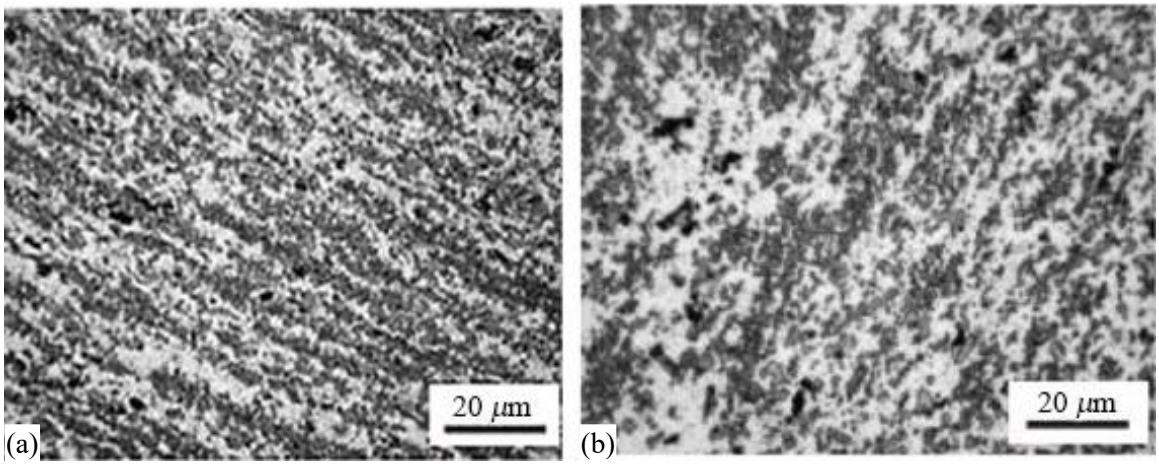

Figure 9. Displays RDECAP micrographs of Al–Si alloys: (a) after 8 cycles and (b) after 16 cycles at 300 °C [17].

Consequently, the die is ready for the next cycle without extracting the sample, as presented in Figure 8(c). If heating is required between two consecutive cycles, a movable furnace is used to raise the entire die assembly to the desired temperature [16]. Nevertheless, a key limitation of this method is that only a small strain is imparted to the specimen during each cycle. Consequently, multiple passes are necessary, making the process both time-consuming and demanding. Figure 9 presents the microstructures of aluminum–silicon alloys subjected to RD-ECAP processing, particularly after 8 and 16 cycles at 300 °C following T6 heat treatment. The microstructures show that silicon particles and intermetallic phases are more uniformly distributed within the aluminum matrix compared to the as-cast alloy. Moreover, the homogeneity of particle distribution improves as the number of RD-ECAP cycles increases from 8 to 16 at 300 °C, as illustrated in Figures 9(a) and (b), respectively [17].

Side Extrusion (SE)

The SE method operates on the same fundamental principle as the rotary-die ECAP technique, and both methods utilize route (A) to introduce strain into the specimen without rotation. This technique incorporates movable punches capable of exerting adequate force on the sample, as illustrated in Figure 10. These punches are powered and regulated by an electrohydraulic system that controls their displacement. The specimen is transferred from channel A to channel B through side extrusion, while punches C and D stay stationary. The control system advances punch A at a uniform speed, while punch B applies a predetermined lateral pressure to the specimen during deformation. In the following cycle, the roles of punches A and B are interchanged, and the process is repeated, eliminating the need to remove the sample from the die. However, a major drawback of this technique is the high expense and complexity associated with its control system [18].

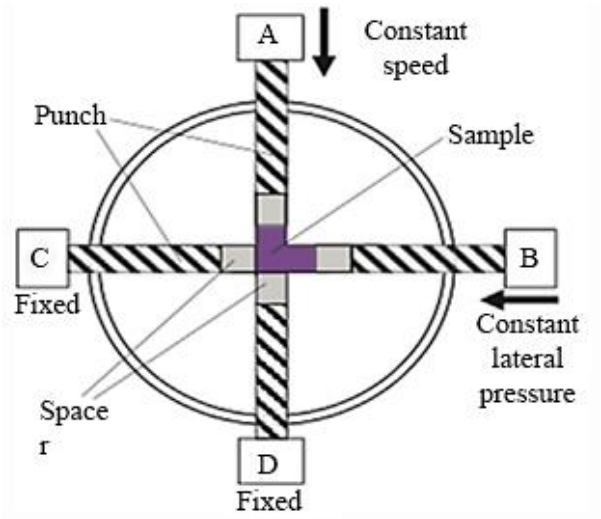

Figure 10. Depicts the side-extrusion ECAP technique [18].

Torsional-ECAP (T-ECAP)

The authors employed the ECAP method to create innovative approaches for consolidating aluminum and copper powders. By integrating ECAP with torsional extrusion (TE), they successfully consolidated pure aluminum powders into fully dense bulk materials using a specially designed ECAP configuration. This method, referred to as T-ECAP, incorporates rotation of the outlet channel during the ECAP process, producing high-density samples with refined grain structures at lower deformation temperatures. Additionally, extrusion in the final stage of deformation increases the strain applied to the specimen compared with conventional ECAP. A schematic illustration of the T-ECAP process is shown in Figure 11 [19,20].

Back pressure ECAP

Previous studies [21] have shown that the strain and stress non-uniformity in specimens processed by conventional ECAP is influenced by die geometry and the type of material. Such non-uniform deformation may promote surface cracking and ultimately cause fracture during the ECAP process. To overcome this problem, several strategies have been adopted to enhance deformation uniformity, including pre-straining and the application of back pressure (as illustrated in Figure 12) [22]. In a study on fabricating a solid tubular specimen from magnesium particles using ECAP with back pressure, the corner gap between the die and the sample shown in Figure 13(a) was removed upon applying back pressure, as illustrated in Figure 13(b). It was found that shear deformation combined with imposed hydrostatic pressure on the specimen produced a uniform distribution of stress and strain in the final product. This approach also delayed fracture during the ECAP process by increasing compressive hydrostatic stresses [21,23].

Expansion ECAP

Figure 14 (1–4) presents a schematic of the Expansion ECAP technique and the resulting product before it is separated from the die. Unlike conventional ECAP, this method incorporates a spherical cavity at the junction of the inlet and outlet channels, serving as back pressure behind the specimen. This modification offers benefits, including the application of higher stresses and improved deformation uniformity. The equivalent strain imposed during the expansion and extrusion stages is given by Eq. (3), which defines the relationship between the material's equivalent strain under an applied force or load and several contributing factors. These factors include the material's initial length, the number of processing cycles, and the ratios of its final diameter to its initial diameter, denoted as and , respectively, as follows:

$$\varepsilon = 4ln\frac{D_I}{D_O} \tag{3}$$

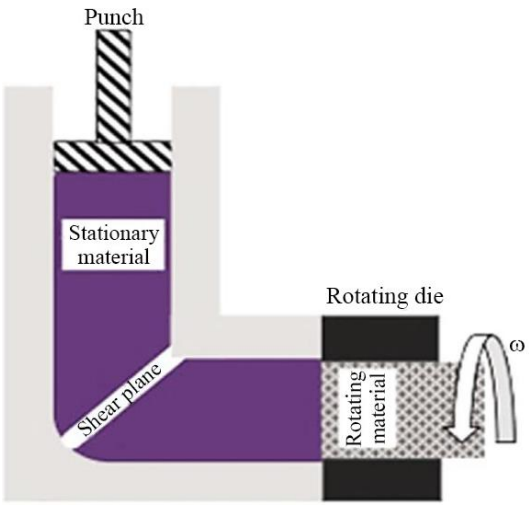

Figure 11. Shows the Torsional ECAP setup [20]

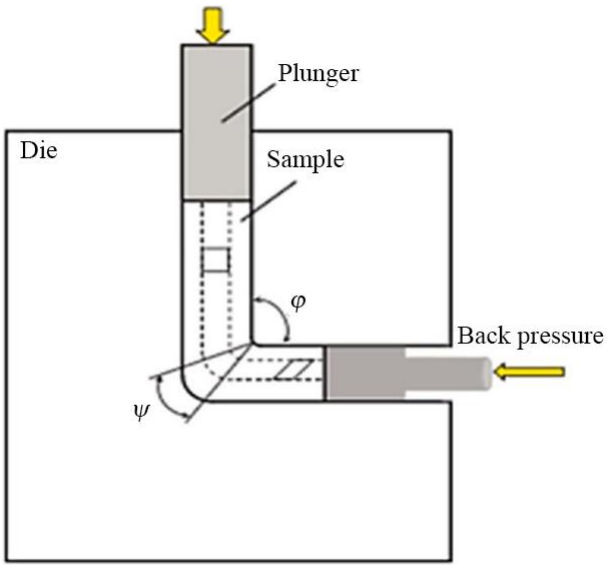

Figure 12. Shows a schematic of the ECAP process with back pressure technique [21].

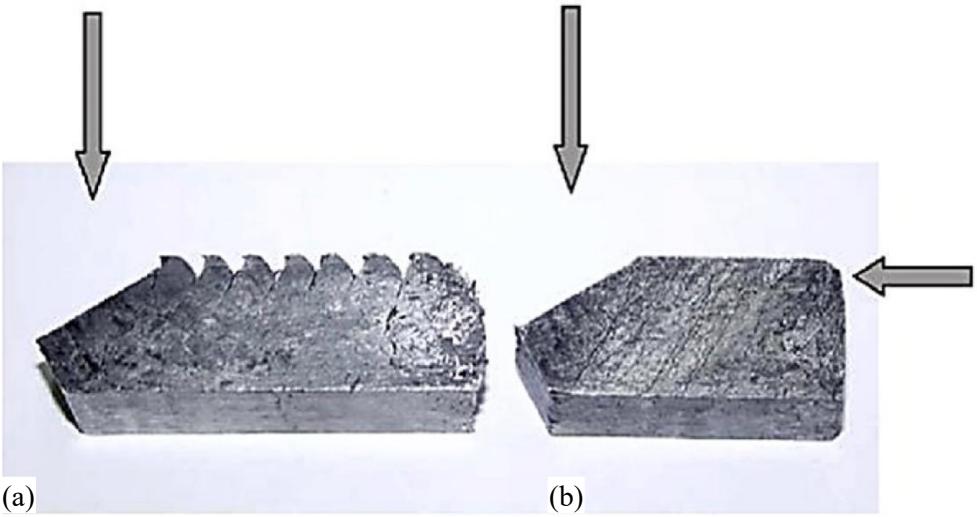

Figure 13. Displays ECAP-processed compacted magnesium alloy particles:
(a) without back pressure and (b) with 60 MPa back pressure [24].

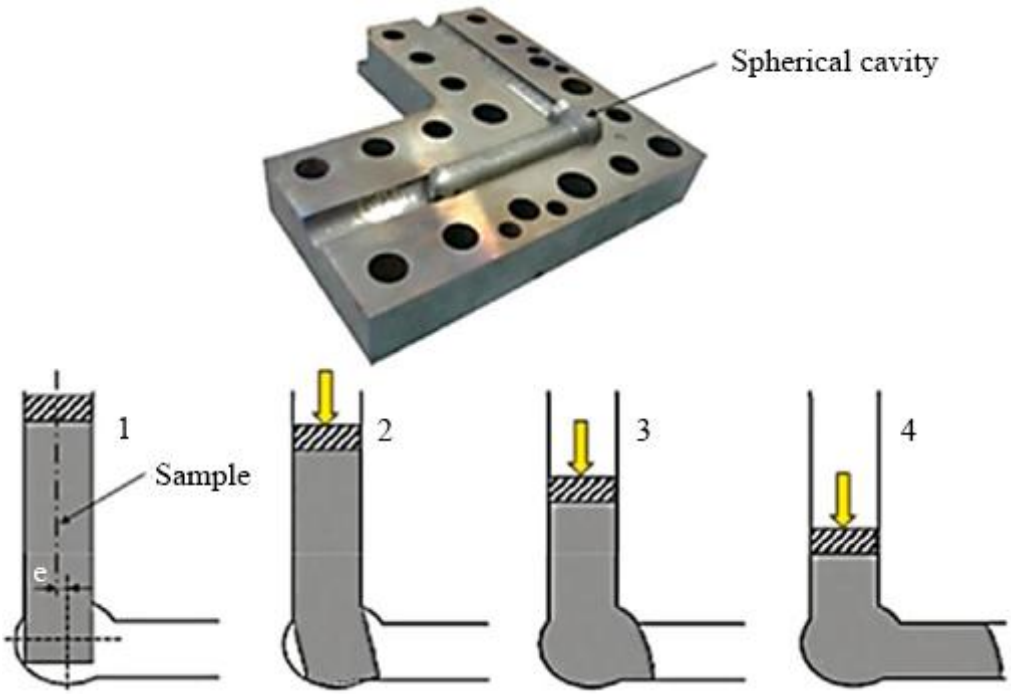

Figure 14. Depicts the Exp-ECAP method, showing half of the die containing the deformed material and the four stages of a processing cycle [21].

In this method, improved grain refinement is attained for the same number of cycles, as the total plastic strain exceeds that of conventional ECAP [21].

ECAP with Parallel Channels

The modified ECAP design is illustrated in Figure 15. In this setup, the inlet and outlet channels are parallel, forming an angle φ. During the ECAP process, the sample is forced through two intersecting channels of equal cross-section, exposing the material to severe plastic strain via simple shear. Shear stress is applied along the N direction across two shear planes. Under frictionless conditions, the equivalent shear strain (γ) in the deformed specimen is calculated using Eq. (4) [26].

$$\gamma = 2cot\left(\frac{\Phi+\Psi}{2}\right)+\Psi cosec\left(\frac{\Phi+\Psi}{2}\right) \tag{4}$$

The effective strain magnitude (ε) after N passes is calculated using Eq. (5)

$$\varepsilon_{eq}=\frac{N}{\sqrt{3}}cot\left(\frac{\Phi+\Psi}{2}\right)+\Psi cosec\left(\frac{\Phi+\Psi}{2}\right) \tag{5}$$

This technique has been effectively used for up to four cycles on copper and titanium. Microstructural investigations reveal that the refined grains in these samples are identical to the ultrafine grain structure obtained after eight cycles of ECAP techniques.

Different Die Designs of ECAP

Conventional ECAP faces challenges such as high energy consumption caused by friction between the die and sample, resulting in non-uniform mechanical properties and poor surface quality. To mitigate this, researchers have developed dies with movable walls (Figure 16) to lower frictional forces. Two die configurations are employed: one with a movable inlet channel (A) and another with a movable wall at the outlet channel (B). Nonetheless, these designs still have limitations, including material extrusion between the components. Other design alternatives involve employing solid steel dies or adjusting the die corner with a tilt angle (α) ranging from 2° to 5° (Figure 17(b)) to minimize cracking and enhance compressive stress.

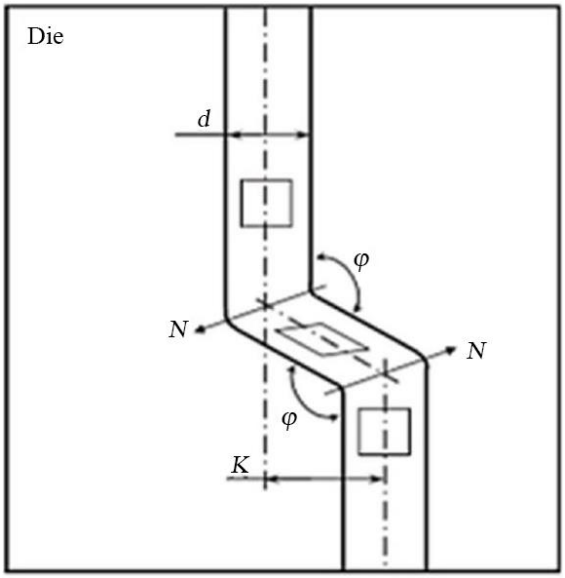

Figure 15. Shows the ECAP process using a parallel-channel die design, with N indicating the direction of the shear planes and K representing the displacement between the two channels [25].

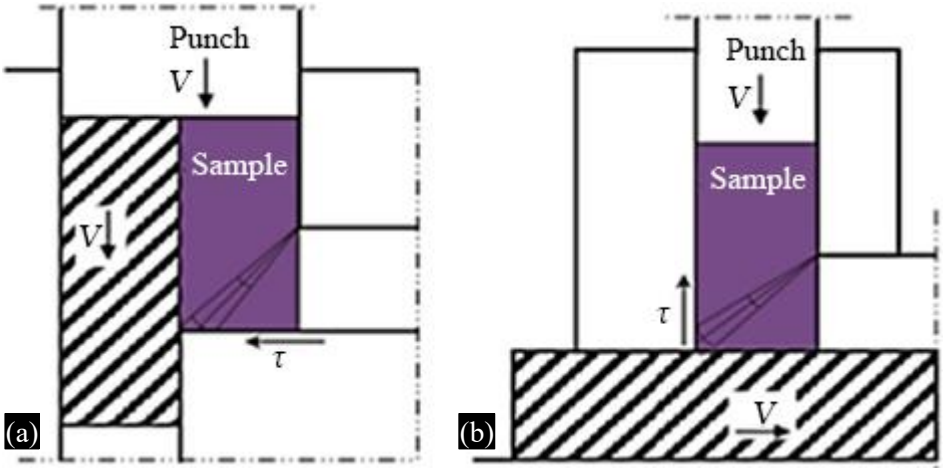

Figure 16. Shows the ECAP principle with adjustable die walls (shaded): (a) in the inlet channel and (b) in the exit channel [28].

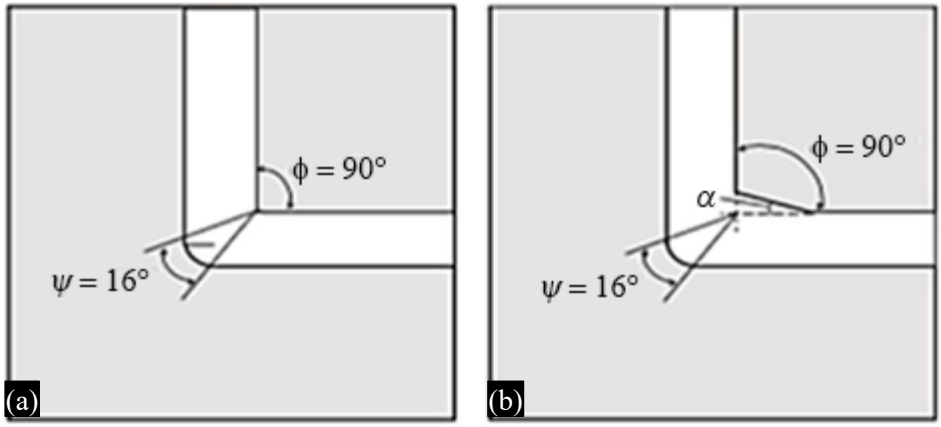

Figure 17. Shows different ECAP die configurations: (a) conventional design and (b) modified design [29].

Dual Equal Channel Lateral Extrusion (DECLE)

Figures 18(a) and (b) illustrate the DECLE method, in which a punch extrudes a billet through a vertical T-shaped inlet channel into a horizontal channel of the same inlet dimensions [30].

Channel Angular Pressing with Converging Billets

Figure 19 shows this method, where two identical punches compress the input billets and merge them into a single output channel, lowering processing force and friction. However, billet adhesion creates issues during separation [31].

Non-equal Channel Angular Pressing (NECAP)

NECAP (Figure 20) is favored over ECAP because it offers a higher extrusion ratio, resulting in a greater processing load and 38% higher strain [32]. NECAP achieves improved grain refinement and a more uniform microstructure, particularly in hard-to-deform alloys, and is also capable of joining dissimilar metals [33]. Figure 21 presents microstructural images of as-cast AZ80 Mg alloy and processed samples at different temperatures and velocities, demonstrating the influence of temperature on dynamic recrystallization [32].

Torsion Extrusion (TE)

The Torsion Extrusion (TE) method, introduced in 2006, is a modification of the conventional high-pressure torsion technique. Figure 22 presents a schematic of the TE process, where the material is

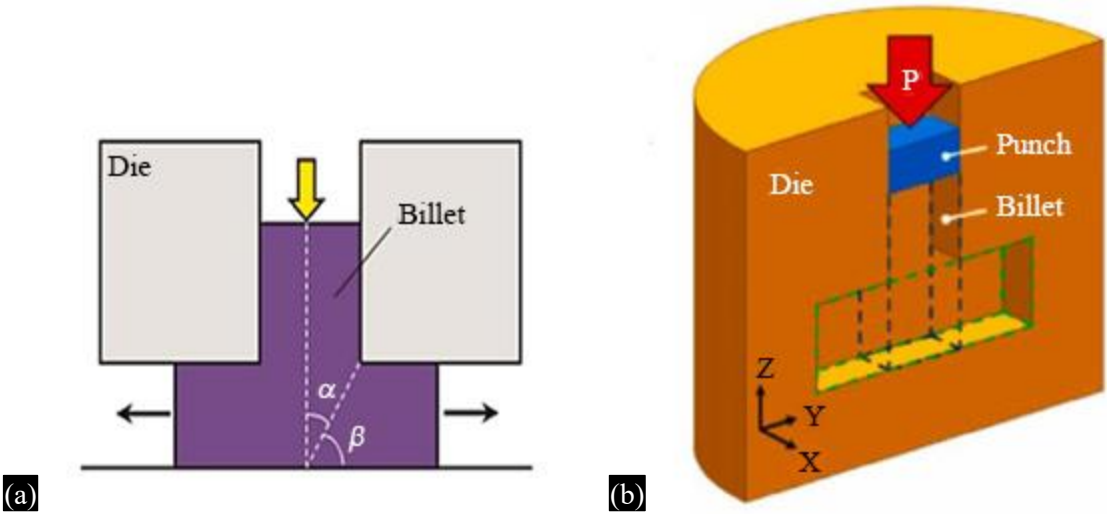

Figure 18. Dual equal-channel lateral extrusion (DECLE) diagram [30].

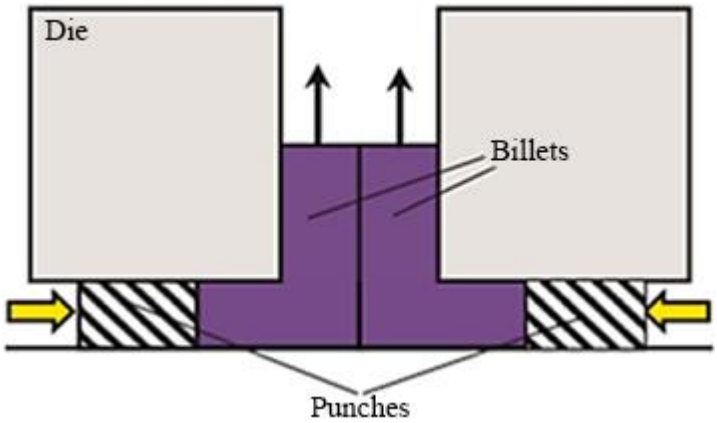

Figure 19. Schematic illustration of channel angular pressing with converging billets [31].

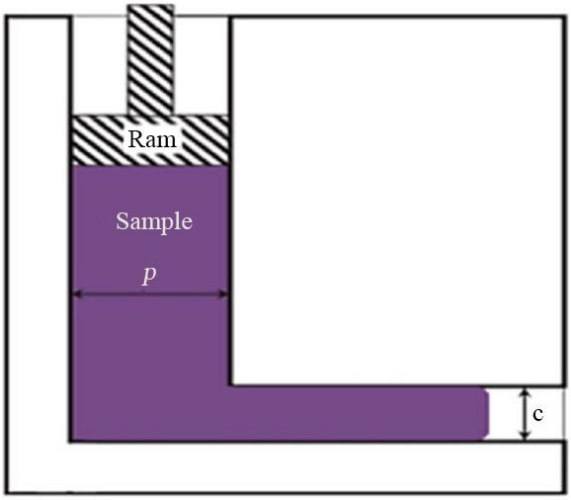

Figure 20. NECAP die Schematic [32].

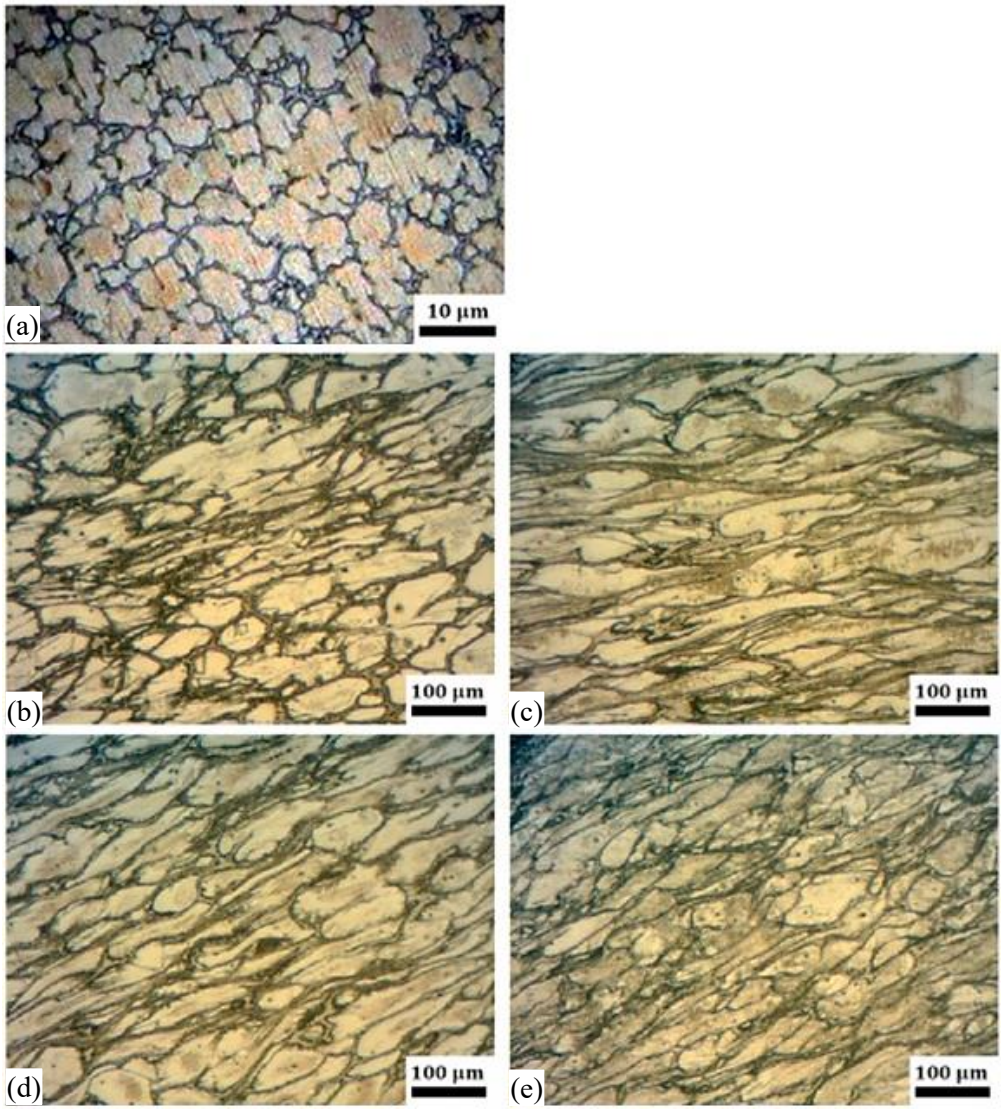

Figure 21. Micrographs of AZ80 Mg alloy: (a) as-cast, and the longitudinal section of NECAP-processed samples under various conditions: (b) T = 250 °C, v = 1 mm/min, (c) T = 300 °C, v = 1 mm/min, (d) T = 300 °C, v = 2 mm/min, and (e) T = 300 °C, v = 4 mm/min [32].

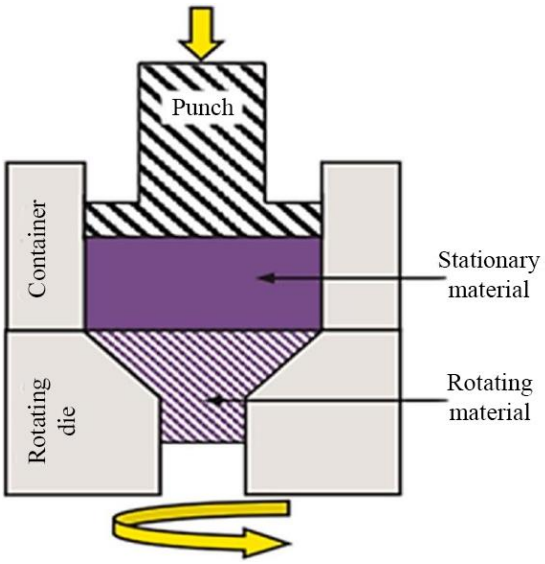

Figure 22. Schematic representation of the torsion extrusion process [34].

extruded through sectional containers that rotate relative to each other, applying high strain to the metal. The extrusion die can be circular, square, or elliptical in shape. The average strain magnitude can be determined using Eq. (6).

$$\varepsilon = \frac{4\pi RN}{3\sqrt{3}H} \tag{6}$$

Here, R and H represent the specimen's radius and length, respectively, while N denotes the number of rotations. The sample experienced greater strain compared to that produced by the conventional extrusion process, as reported in a previous study [34].

Multiple Direct Extrusion (MDE)

The MDE technique was developed from the direct extrusion method. In this approach, illustrated in Figure 23, the specimen is extruded into a rectangular die with a 50% reduction ratio. After each extrusion cycle, the extruded product is cut at the output ends and reassembled to restore the original cubic shape of the billet, after which the extrusion process is repeated. For the subsequent cycle, two options exist: either no rotation or a 90° rotation around the longitudinal axis of the original billet [35]. In MDE, as the material moves through the discontinuity zone, newly formed grains become misoriented along the shear planes. Shearing begins when the elongated grains are sufficiently thinned, and tangential stress is applied at the surface of the velocity discontinuity, as illustrated in Figure 24 [36].

Accumulated Extrusion (AE)

The AE process, shown in Figure 25, is similar to the MDE method but generates higher strain than that achieved in successive MDE cycles. In AE, the original billet is cut into several identical sections, which are stacked, extruded to the final size, and the cycle is repeated. This technique is used to produce multilayer plates. However, a key challenge for both MDE and AE methods is ensuring proper bonding and adhesion between the stacked layers [37].

Pure Shear Extrusion (PSE)

The PSE process enables combined modes of simple and pure shear deformation without the repeated working that typically causes inhomogeneous deformation. As shown in Figure 26, different deformation zones exist in the die, with the sample being compressed in the central zone. This approach imposes high plastic strain on the specimen, achieving the desired plastic deformation. PSE allows adjustment of the pure-to-simple shear ratio by altering the sample shape from square to rhombic during deformation [37]. A key advantage of this method is the ability to produce relatively large ultrafine-grained samples without the need for back pressure or sample rotation [38].

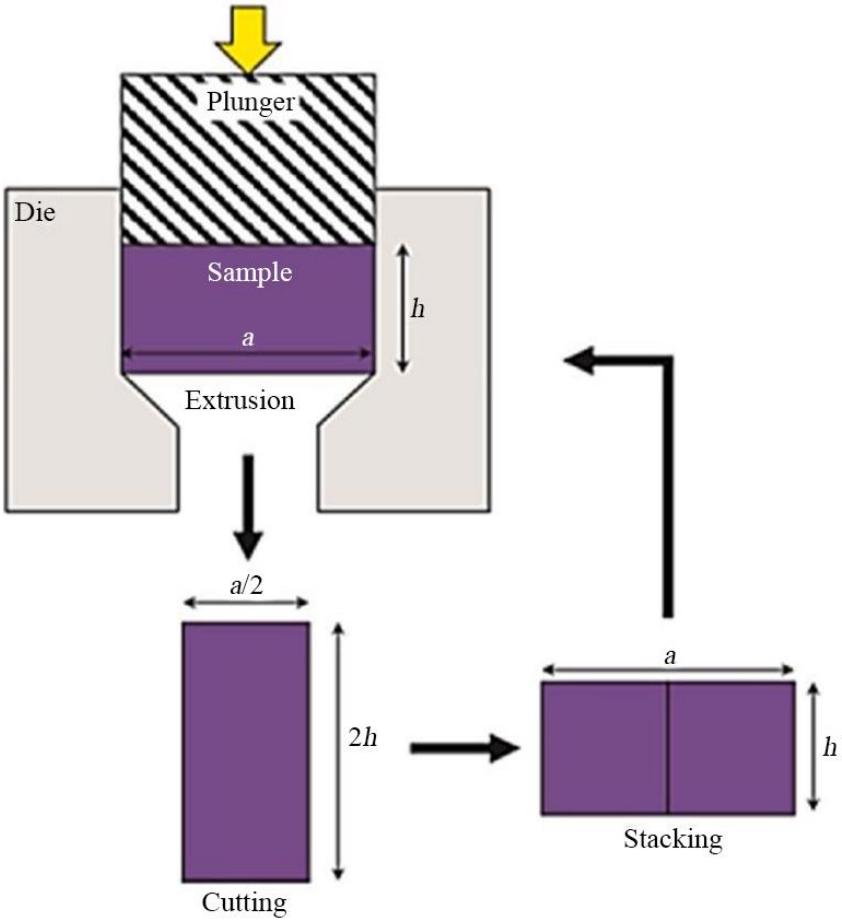

Figure 23. Representation of multiple direct extrusion process [35].

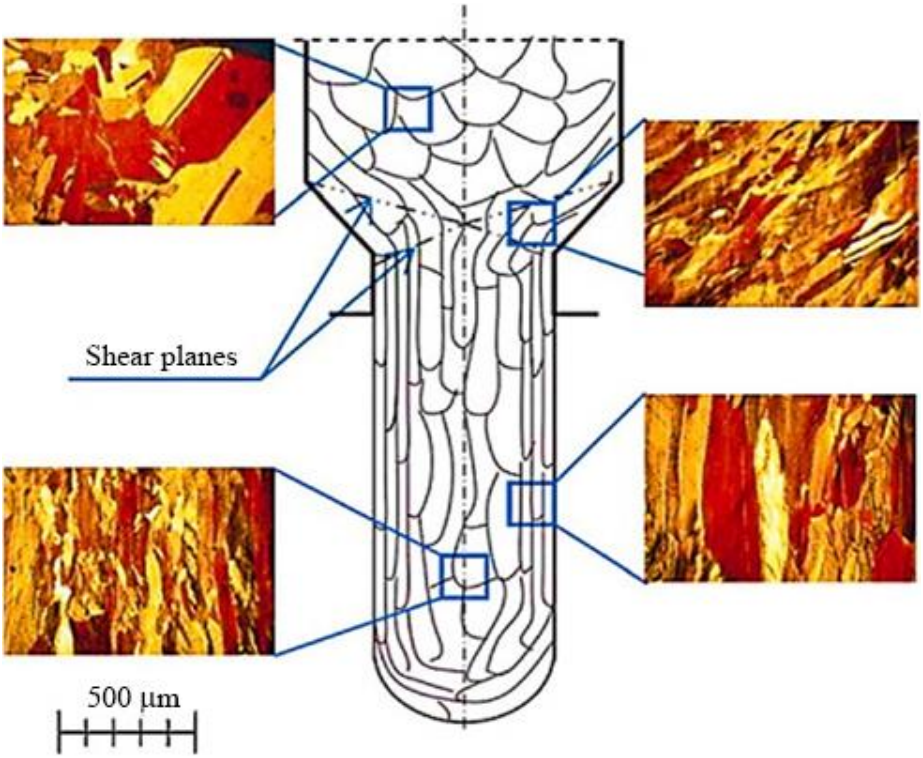

Figure 24. Optical micrographs of processed copper by MDE after one pass [36].

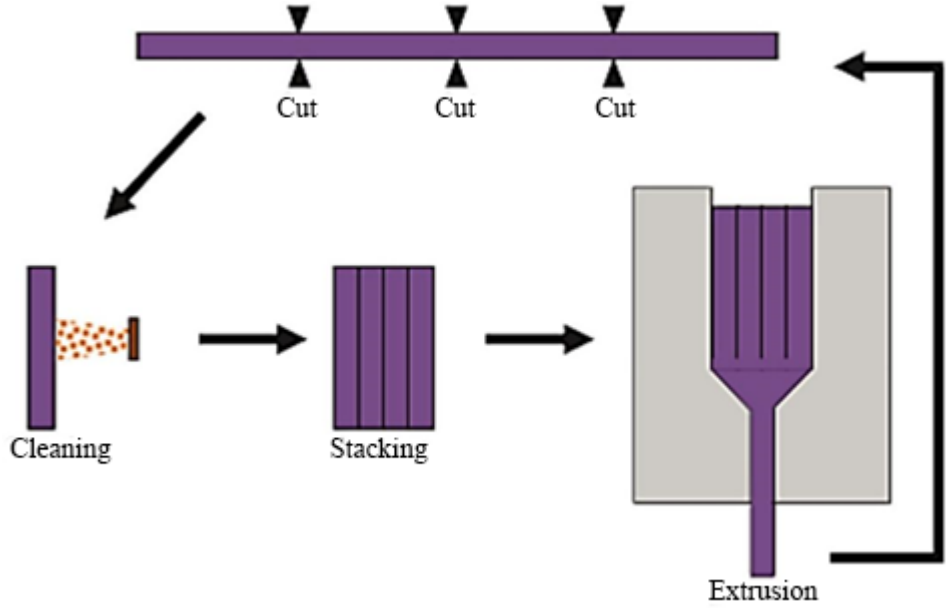

Figure 25. AE process schematic [37].

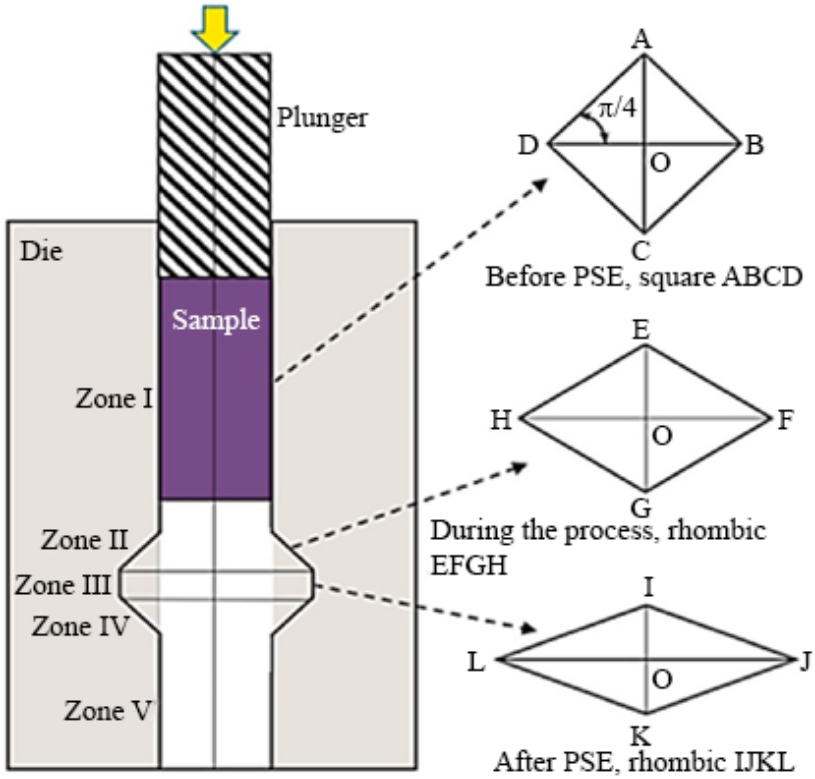

Figure 26. Diagrammatic representation of pure shear extrusion and the changes in the specimen's cross-section at the midpoint of PSE deformation [38].

C-shape Equal Channel Reciprocating Extrusion (CECRE)

The CECRE technique, illustrated in Figure 27, is based on applying shear stress through cyclic deformation. The proposed CECRE method not only surpasses the benefits of cyclic extrusion compression (CEC), multidirectional forging (MDF), and equal channel angular extrusion (ECAE) but also addresses the strain variation between the center and peripheral regions that occurs in ECAE, MDF, and CEC processes. Additionally, it can impose shear strain without altering the sample size [39].

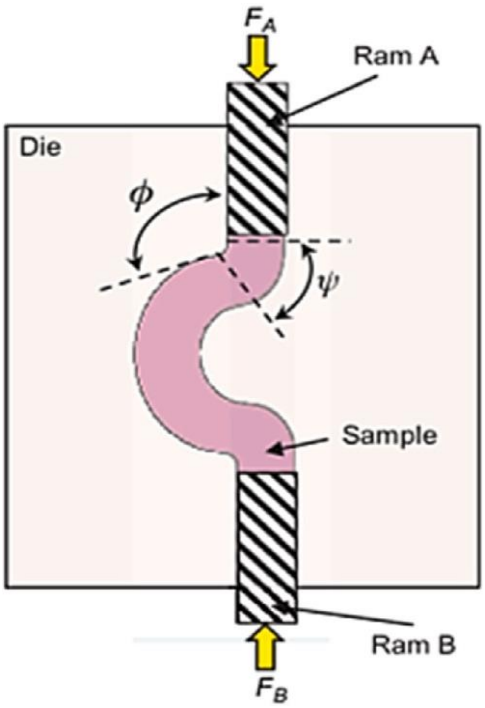

Figure 27. A schematic illustration of the (CECRE) method [39]

Twist Extrusion (TE)

The TE mechanism, illustrated in Figure 28, involves extruding the sample through a twisted die. The strain variation from the surface to the center influences the grain size of the specimen. The asymmetrical products generated by the TE method restrict its use to rectangular samples. Consequently, the TE technique is unsuitable for producing industrial-scale samples due to buckling and the limited travel distance of the plunger. Consequently, two new methods derived from TE—Elliptical Cross-Section Spiral Equal Channel Extrusion and Planar Twist Extrusion—have been developed to overcome TE's limitations. These modifications enhance plunger stability, decrease frictional forces, and enable the production of longer ultrafine-grained samples [40].

Repetitive Upsetting (RU)

The RUE process, illustrated in Figure 29(a) and (b), applies compressive forces to a disc-shaped sample. The specimen is introduced into the die through an upper channel using a plunger, as shown in Figure 29(c). After each pass, it is removed from the bottom of the die, rotated, and then reinserted for the next pass [41]. By reducing the sample thickness, the RUE method can produce industrial-scale thin plates, especially for hard materials such as magnesium alloys [42], making it suitable for commercial applications. The refined grains, illustrated in Figure 30, decrease from 80.45 μm in the original billet (Figure 30(a)) to smaller, more uniformly distributed grains in Figure 30(b) and (c), reaching 4.08 μm after four passes (Figure 30(d)). The transverse material flow in multiple directions, resulting from increased deformation during RUE, enables the development of a homogeneous microstructure [43].

Cylinder Covered Compression

The method outlined in the paragraph was developed to overcome the challenge of producing ultrafine-grained materials without cracking in hard-to-deform alloys, such as spheroidal cast iron. The procedure consists of multiple steps, as illustrated in Figure 31. In this process, steel cylinder specimens are first hot-compressed, then cut into equal sections, with surface layers machined off. The sections are stacked, placed into a cylindrical die, and hot-compressed again. This technique has been successfully applied to spheroidal cast iron, achieving a 99.2% reduction in height [44].

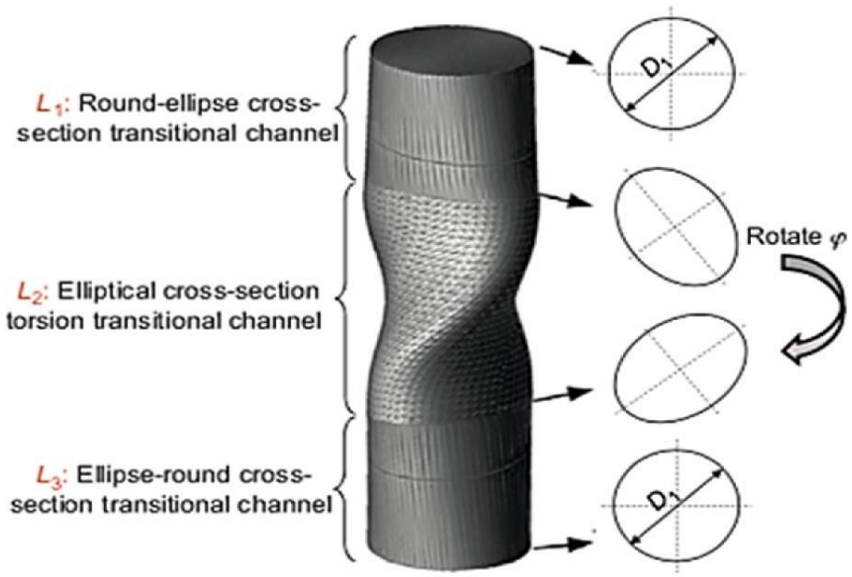

Figure 28. Schematic diagram of ECSEE and PTE [40].

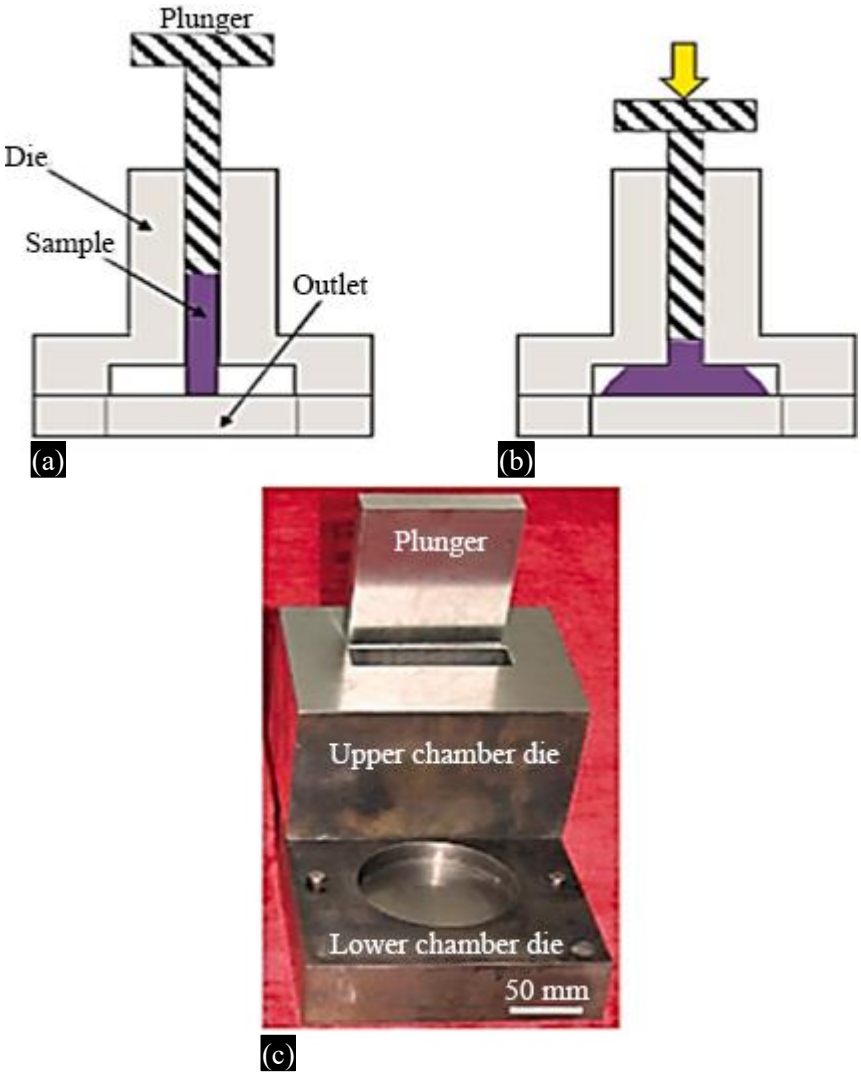

Figure 29. Illustration of the RUE process: (a) initial stage, (b) during the process, and (c) die setup [41].

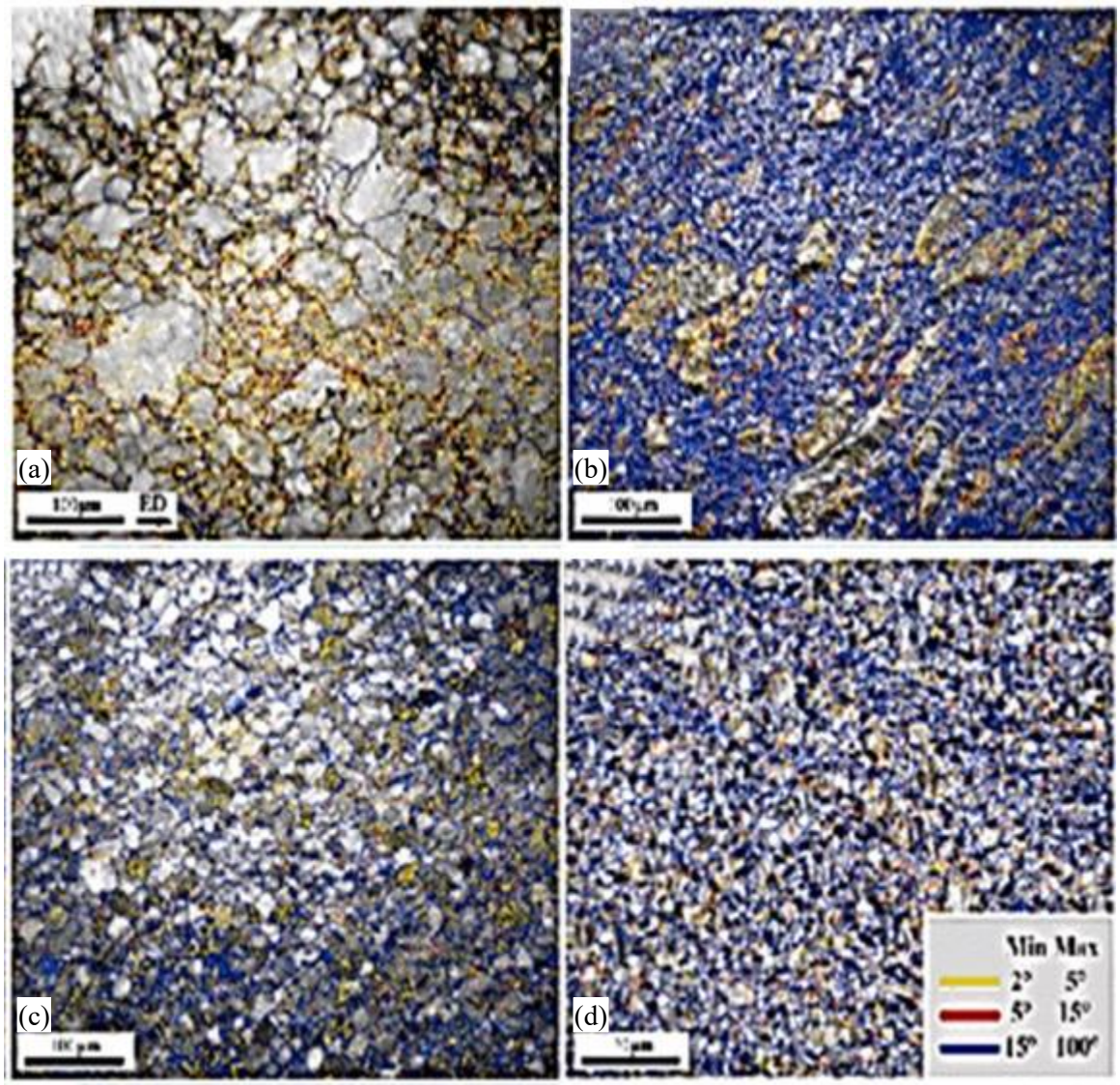

Figure 30. Grain boundaries in an alloy processed by RUE after multiple passes [41].

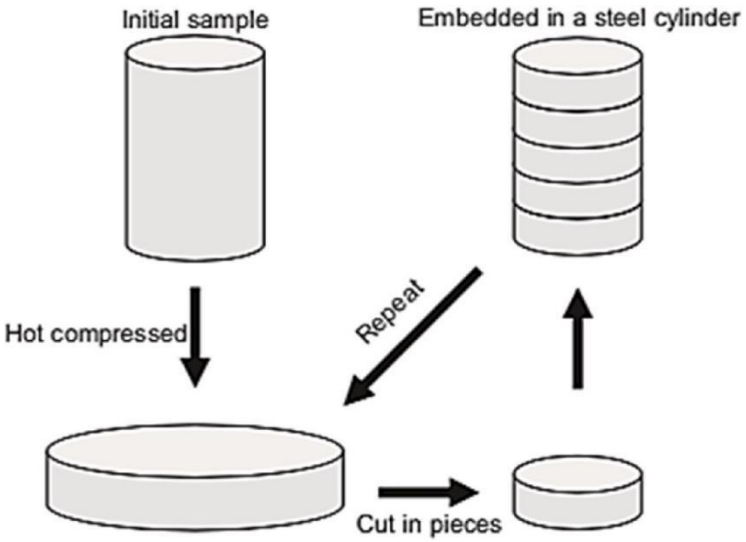

Figure 31. A diagrammatic illustration of the CCC technique [44].

Repetitive Upsetting and Extrusion (RUE)

The RUE mechanism is shown in Figure 32, where a circular rod undergoes an upsetting step followed by extrusion. These upsetting and extrusion operations are repeated until the desired number of cycles is achieved. RUE offers several benefits, including the ability to impose high strain per cycle, which leads to more efficient grain refinement without the need for additional machining of the specimens. Additionally, warm deformation below the recrystallization temperature can be applied prior to the upsetting step to enhance the workability of hard materials. The primary drawback of this method is that during the upsetting stage, tensile stresses develop on the outer surface, which can lead to cracking and decreased material workability [45].

Cyclic Extrusion and Compression (CEC)

The CEC method is illustrated in Figure 33, where the specimen is pushed into the reduced-diameter channel of the die by ram A, which has a smaller diameter, while a back-extrusion force (FB) is applied to the extruded material to restore it to its original dimensions. While CEC is effective for processing hard metals because of the compressive stress state, some materials may enter the gaps, increasing the process load and stress. Another limitation of the CEC method is the restriction on specimen length, as high friction elevates the processing load and can cause buckling or yielding of the punch or ram [46,47].

Cyclic Expansion and Extrusion (CEE)

The stages of the CEE process are depicted in Figure 34. Initially, the main punch blocks the outlet channel, causing the material to flow radially and fill the barrel zone, as shown in Figure 34(a) and (b). The following extrusion step begins when the upper punch is pushed after the primary punch is removed, supplying the required back pressure for material expansion, as illustrated in Figure 34(c). The process can be repeated for additional passes without removing the sample from the die. Furthermore, the entire die is rotated by 180° (Figure 34(d)). This technique can achieve strain levels up to 4 and allows for any number of passes. The microstructure of an annealed sample processed

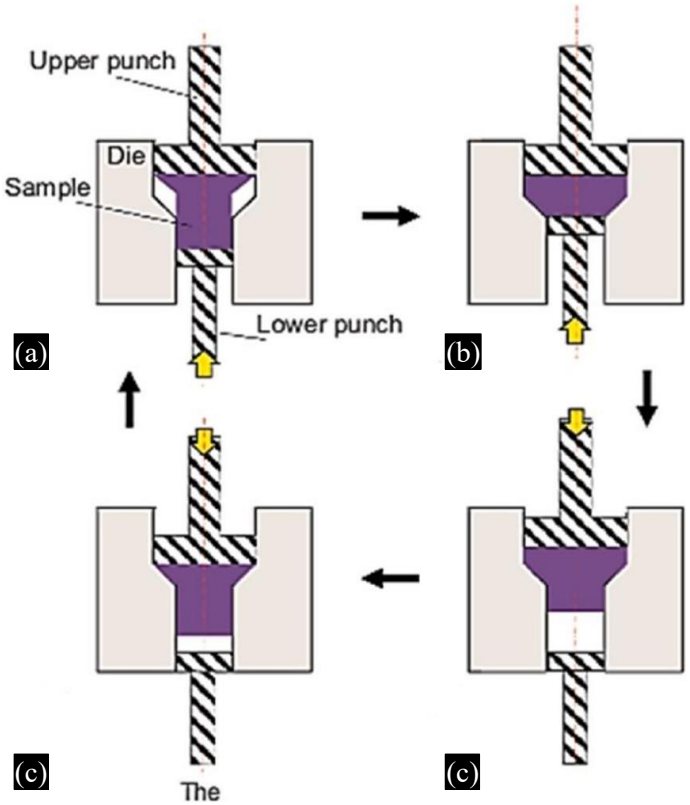

Figure 32. A schematic illustration of RUE method [45].

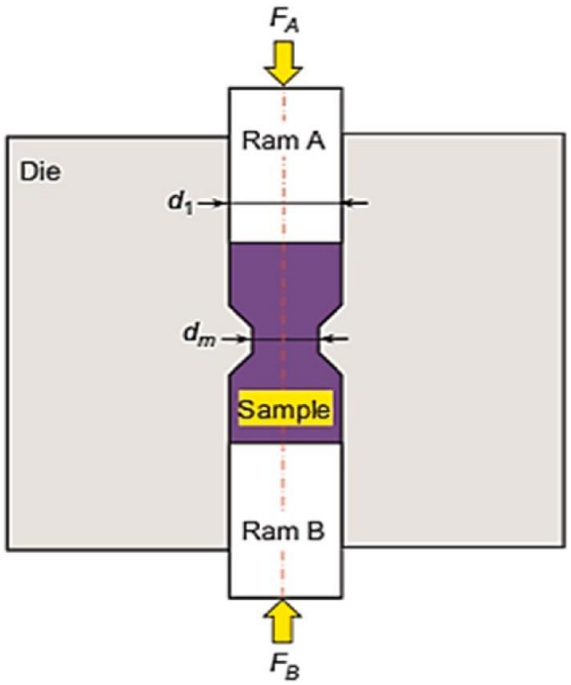

Figure 33. Configuration of the CEC die [46]

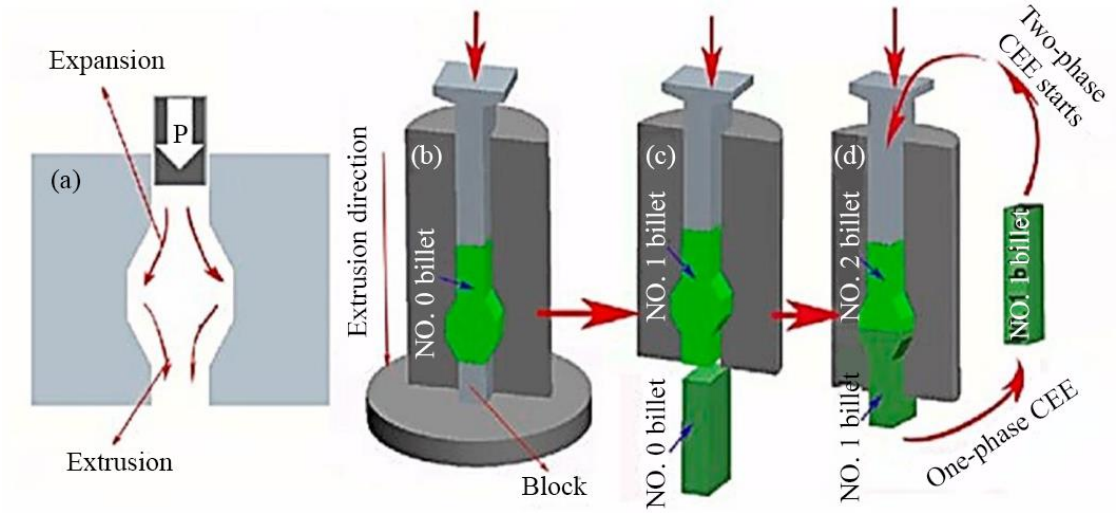

Figure 34. Schematic representation of the CEE stages [48]

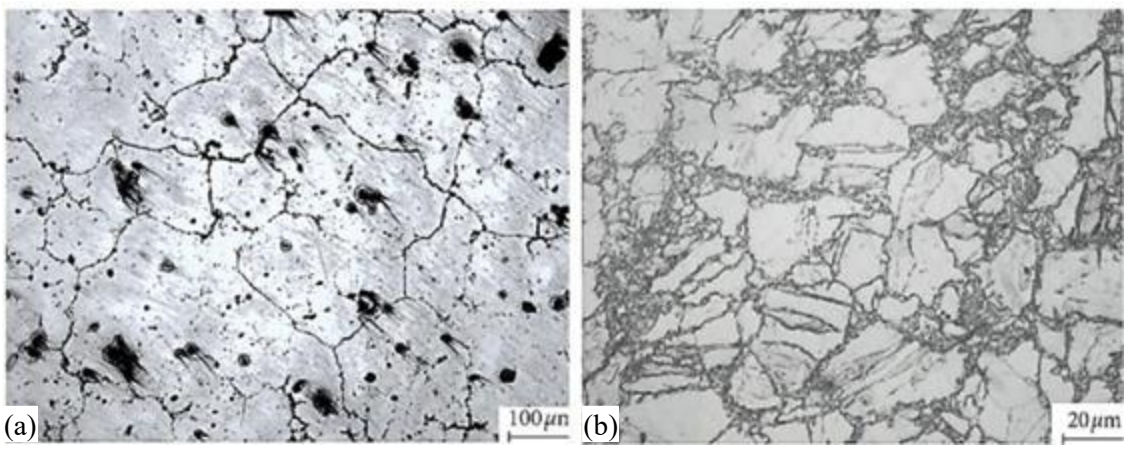

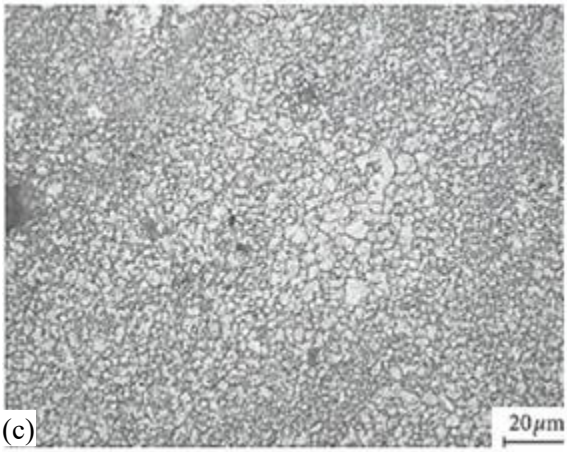

Figure 35. Optical microstructure images of: (a) the annealed sample; (b) one CEE pass; (c) two-passes CEE [49]

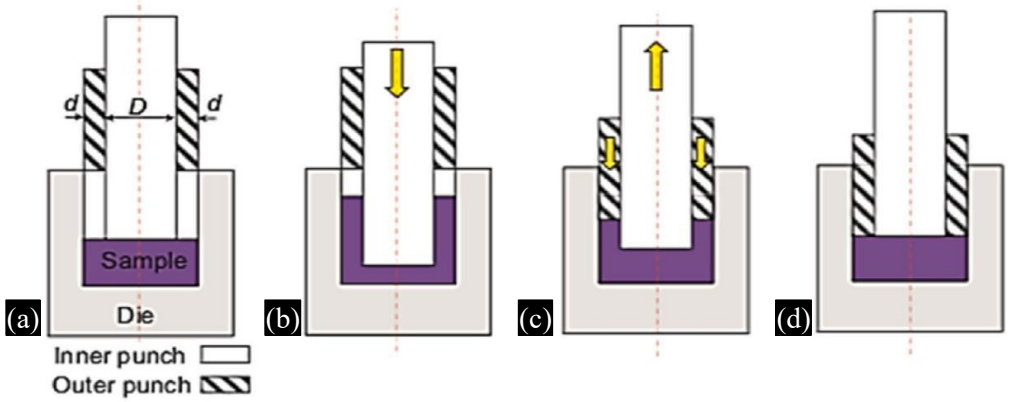

Figure 36. Flow diagram of the ABE process: (a) start of the cycle, (b) back extrusion, (c) back compression, and (d) completion of the cycle [50].

using the CEE method is shown in Figure 35(a). Optical micrographs after one and two passes are presented in Figure 35(b) and (c), respectively. This method allows samples to undergo a predetermined number of passes without being removed from the die until the process is complete. Additionally, unlike CEC, no external back-pressure system is needed, as the extrusion force itself generates sufficient back pressure for material expansion [48,49].

Accumulative Back Extrusion (ABE)

The ABE technique is employed to fabricate tubular samples of different sizes. The schematic of the ABE process is shown in Figure 36(a), where the specimen is back-extruded into the space created by the inner punch (Figure 36(b)), then compressed back by the outer punch (Figure 36(c)), completing the cycle (Figure 36(d)). This method is capable of processing large-diameter samples; however, it cannot produce long specimens with uniform microstructures and mechanical properties [50]. The cyclic forward and backward extrusion (CFBE) technique is used to fabricate ultrafine-grained bulk materials under very high strains [50]. As illustrated in Figure 37(a), the CFBE process employs a dual-punch setup for forward and backward extrusion, followed by a back-pressure step shown in Figure 37(b).

Accumulative Compression Bonding (ACB)

The ACB process generates bulk nanostructured metals, as illustrated in Figure 38. In this method, the specimen is compressed within a channel die, resulting in a plane strain compression bonding known as ideal rolling deformation. During this process, the sample's thickness is reduced while its

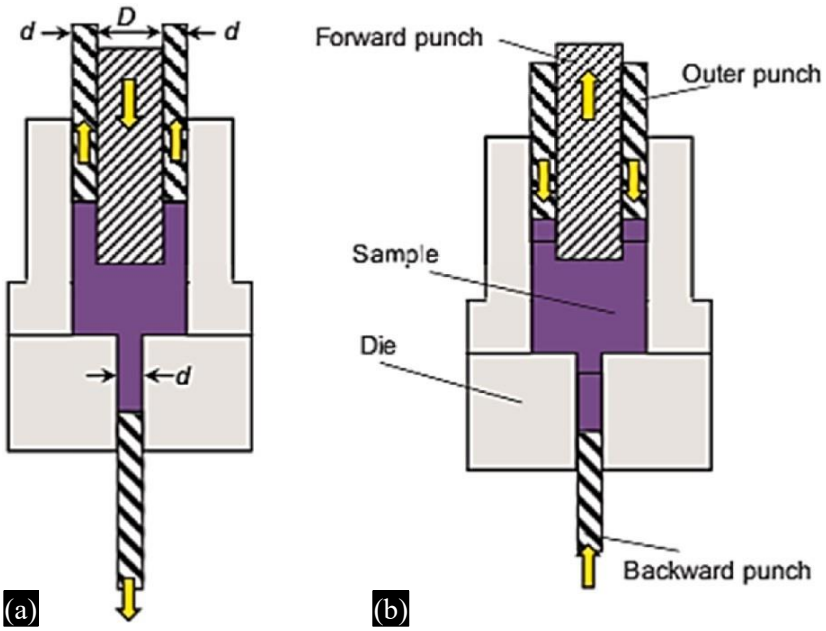

Figure 37. CFBE method: (a) first half-cycle, (b) second half-cycle [50].

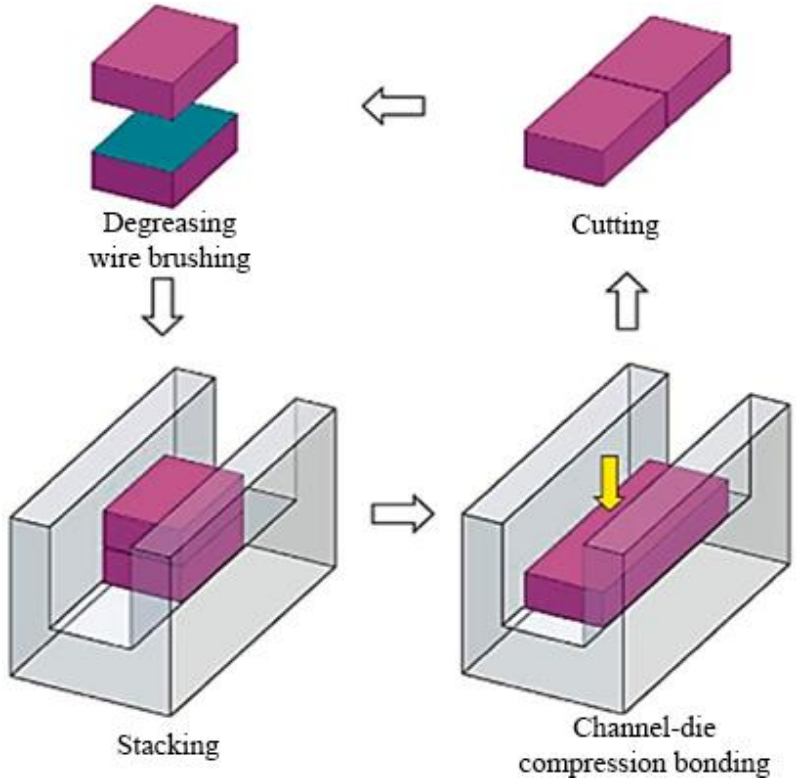

Figure 38. A schematic representation of (ACCB) [51].

length increases within the channel die, with no lateral spreading occurring. To restore the original thickness, the sample is first wire-brushed and degreased, then cut into two halves and stacked. In the channel die, the stacked billets are compressed by 50% during the subsequent cycle to create a bulk sample with sufficient bonding. The ACB process can be used to produce homogeneous ultrafine-grained metals as well as high-strength metal matrix composites (MMCs). This procedure can be performed using a channel die attached to a standard pressing machine, eliminating the need for a high-capacity rolling mill. Additionally, it is suitable for large-sized samples, and the strain can be

accurately controlled by adjusting the pressing speed and deformation amount [51]. A previous study investigated the effects of strain accumulation and annealing on the interfacial and grain structures (Mg and Al_3Mg_2 layers) of an Al/Cu/Mg multilayered composite produced via the accumulative roll bonding (ARB) process. The results showed that strain accumulation promoted the development of a uniform interfacial microstructure and refined grain structure. Subsequent annealing further enhanced the grain structure and removed defects at the interface. Overall, the study indicates that the ARB process, combined with strain accumulation and annealing, can produce a composite with superior mechanical properties [52].

Combined Severe Plastic Deformation Methods

Certain previously described techniques can be combined to achieve greater advantages, leading to enhanced material properties and increased process efficiency. These hybrid approaches can impose higher equivalent strains on materials while also addressing some of the limitations associated with Severe Plastic Deformation methods [52]. Cold rolling followed by ECAP and HPT has been shown to enhance mechanical properties. Another study combined two Severe Plastic Deformation techniques, ECAP and extrusion, to produce ultrafine-grained materials such as pure nickel and Al–Mg alloys.

CONCLUSIONS

There are multiple techniques available to induce severe plastic deformation in metals to enhance their mechanical properties and microstructure. Conventional methods like rolling, forging, and extrusion are limited in the amount of strain they can impart, whereas advanced techniques such as ECAP, HPT, and related processes can achieve much higher strains and result in much finer microstructures. However, these techniques also suffer from certain limitations, including high energy requirements, constraints of the equipment, and challenges in manufacturing large-sized samples.

To address these limitations, researchers have suggested improvements to existing methods, including the use of multiple passes, alterations in die design, the development of new techniques, or the sequential combination of two or more Severe Plastic Deformation processes.

These modifications can enhance process efficiency, lower energy consumption, and lead to improved mechanical properties and microstructural characteristics of the material. Nevertheless, each technique has its own benefits and constraints, and the selection of an appropriate method depends on the material being processed and the targeted properties.

Overall, recent advances in Severe Plastic Deformation techniques have demonstrated significant potential for enhancing the mechanical properties and performance of metals across a wide range of applications. The technical details of Severe Plastic Deformation discussed in this review can assist researchers in building upon and advancing the outcomes of previous studies.

ECAP is a crucial technique for producing an ultrafine-grained structure and can be used to improve the mechanical properties of magnesium alloys. The behavior of the material after processing is strongly influenced by the ECAP parameters.

Increasing the number of ECAP passes up to four leads to a reduction in the grain size of magnesium alloys. Higher processing temperatures promote longer recovery times, which in turn result in grain coarsening. Additionally, low-angle grain boundaries are formed more predominantly than high-angle grain boundaries.

The ECAP die channel angle has a significant influence on the microstructure of magnesium alloys. Finer grain sizes and improved mechanical properties were obtained by employing a larger die angle, lower processing temperatures, and a higher number of ECAP passes, specifically four passes.

REFERENCES

1. V.Y. Estrin, Extreme grain refinement by severe plastic deformation: a wealth of challenging science, Science direct 61 (3) (February 2013) 782–817.
2. H.S.K.G. Faraji, Review of principles and methods of severe plastic deformation for producing ultrafine-grained tubes, Mater. Sci. Technol. 33 (8) (2017).
3. G.M.M.A. Babaeia, Repetitive forging (RF) using inclined punches as a new bulk severe plastic deformation method, Mater. Sci. Eng. 558 (2012) 150–157.
4. N.J.Q.W.S. Zhao, High density nano-scale twins in Cu induced by dynamic plastic deformation, Science Direct 53 (6) (2005) 745–749.
5. H.S.K.G. Faraji, Review of principles and methods of severe plastic deformation for producing ultrafine-grained tubes 33 (8) (2017).
6. Z. Langdon, Using High-Pressure Torsion for Metal Processing, Fundamental and Applications, 2008, pp. 893–979.
7. T.F.a.Z.H. Edalati, Microstructure and mechanical properties of pure Cu processed by high-pressure torsion, Mater. Sci. (2008) 168. –173.
8. P.W. Bridgman, On torsion combined with compression, J. Appl. Phys. 14 (6) (2004) 273.
9. A. M. H. H. a. Y. I. Dayan Nugmanov, Structure and Tensile Strength of Pure Cu after High Pressure Torsion Extrusion 9 (10) (2019).
10. Y. B. Y. E. Y. I. Roman Kulagin, A mathematical model of deformation under high pressure torsion extrusion, Metals 9 (2019).
11. A. ,. A. B. B. G. Hohenwarter, Technical parameters affecting grain refinement by high pressure torsion, J. Mater. Res. 100 (12) (2013).
12. Y. J. W. Z. H. Mi Iwahashi, Principle of equal-channel angular pressing for the processing of ultra-fine grained materials, Sceince Direct 35 (Issue 2) (1996), 2.
13. W.-S. J. K. K.-T. H. S. Inyoung Kim, Deformation structures of pure Ti produced by equal channel angular pressing, Science direct 45 (5) (2001) 575–580.
14. S.G.M.G.A. Azimi, Mechanical properties and microstructural evolution during multi-pass ECAR of Al 1100–O alloy, Science Direct 42 (2012) 388–394.
15. V. Estrin, Extreme grain refinement by severe plastic deformation;A wealth of challenging science 782–817 (2013), 61.
16. Y. H. A. J.-C. K. Nishida, Rotary-die equal-channel angular pressing of an Al – 7 mass% Si – 0.35 mass% Mg alloy, Scripta Mater. 45 (3) (2001) 261–266.
17. N.S.I.S. Aibin Ma, Effect of Heat Treatment on Impact Toughness of Aluminum Silicon Eutectic Alloy Processed by Rotary-Die Equal-Channel Angular Pressing 45 (2) (2004).
18. K.Z.H.M.N. Nakashima, Development of a multi-pass facility for equal-channel angular pressing to high total strains 281 (1–2) (2000) 82–87.
19. X.K. Xia, Back pressure equal channel angular consolidation of pure Al particles, Scripta Mater. 53 (11) (2005) 1225–1229.
20. B.M.J.M.H. Mani, Consolidation of Commercial Pure Aluminum Powder by Torsional-Equal Channel Angular Pressing (T-ECAP) at Room Temperature, vol. 219, Powder Technology, 2012, pp. 1–8.
21. D.E.B. l Semiatin, The effect of material properties and tooling design on deformation and fracture during equal channel angular extrusion, Acta Mater. 48 (8) (2000) 1841–1851.
22. F.S.S.-B. Saniee, Expansion Equal Channel Angular Extrusion, as a Novel Severe Plastic Deformation Technique, vol. 50, Springer, 2015, pp. 3908–3919.
23. W.Z. LiuZuyan, Finite-element analysis of the load of equal-cross-section lateral extrusion, J. Mater. Process. Technol. 94 (2–3) (1999) 193–196.
24. R. Lapovok, Back pressure in equal channel angular pressing, JOURNAL OF MATERIALS SCIENCE, Russian Metallurgy (Metally) 40 (2005).
25. G.Z.Y.L.Y.G.S. Xu, Numerical studies on processing routes and deformation mechanism of multi-pass equal channel angular pressing processes 167 (2006) 251–259.

26. T.G. Ruslan, Z. Valiev, Principles of equal-channel angular pressing as a processing tool for grain refinement Author links open overlay panel, Prog. Mater. Sci. 51 (7) (2006) 881–981.
27. P. A. S. J. B. K. N. G. R.Manna, Physical modeling of equal channel angular pressing using plasticine, Scripta Mater. 53 (12) (2005) 1357–1361.
28. T.G. ChengXu, Influence of a round corner die on flow homogeneity in ECA pressing, Scripta Mater. 48 (1) (2003) 1–4.
29. W. L. Y. W. L. B. K. C. Shunqi Wang, A modified die for equal channel angular pressing, J. Mater. Process. Technol. 209 (7) (2009) 3182–3186.
30. R.K.B. Talebanpour, Microstructural and mechanical properties of commercially pure aluminum subjected to Dual Equal Channel Lateral Extrusion, Mater. Sci. Eng. 527 (1–2) (2009) 141–145.
31. L.J.M.M.A. Rosochowski, Equal channel angular pressing with converging billets—experiment, Mater. Sci. Eng. 560 (3) (2013) 358–364.
32. R. L. A. H. C. G. Laszl ´ o S.T ´ oth, Non-equal channel angular pressing of aluminum alloy, Scripta Mater. 61 (12) (2009) 1121 ´ –1124.
33. A. M, J. S, M. K, S.P.W. Pachla, Wrought magnesium alloys ZM21, ZW3 and WE43 processed by hydrostatic extrusion with back pressure, ARCHIVES OF METALLURGY AND MATERIALS 57 (2) (2012) 485–493.
34. S. Mizunuma, Large straining behavior and microstructure refinement of several metals by torsion extrusion process, Trans Tech Publ 503–504 (2006) 185–192.
35. C.C.L. Zaharia, Multiple direct extrusion: a new technique in grain refinement, Mater. Sci. Eng. 550 (2012) 293–299.
36. R.R.L. Zaharia, Multiple direct extrusion: A new technique in grain refinement 550 (10) (2012) 293–299.
37. H.S.H.T. GhaderFaraji, Severe plastic deformation methods for bulk samples, Severe Plastic Deformation s. 626 (2018) 423–431.
38. F.M. Ebrahimi, Experimental and numerical analyses of pure copper during ECFE process as a novel severe plastic deformation method, Prog. Nat. Sci.: Mater. Int. 24 (1) (2014) 68–74.
39. H.G.F.E.Z. Torabzadeh, Cyclic Flaring and Sinking (CFS) as a New Severe Plastic Deformation Method for Thin-Walled Cylindrical Tubes, Transactions of the Indian Institute of Metals, 2015.
40. G. R. O. S. S. S.V.Zherebtsov, Production of submicrocrystalline structure in large-scale Ti–6Al–4V billet by warm severe deformation processing, Scripta Mater. 51 (12) (2004) 1147–1151.
41. Q. W. H. Z. W. G. Jianfeng Liu, Microstructure and mechanical properties of NZ30K magnesium alloy processed by repetitive upsetting, J. Alloys Compd. 589 (2014) 372–377.
42. I. B, T. Raghu, Deformation behaviour of bulk materials during repetitive upsetting-extrusion (RUE), Int. J. Material Form. 3 (2010) 267–278.
43. L.Y.W.E.Y. Hu Lianxi, Ultrafine grained structure and mechanical properties of a LY12 Al alloy prepared by repetitive upsetting-extrusion, Mater. Sci. Eng. 422 (1–2) (2006) 327–332.
44. T.Y.J.W.X. Zhao, A new Severe Plastic Deformation process for spheroidal cast iron, Mater. Lett. 58 (19) (2004) 2335–2339.
45. L.H. Yanxiong Liu, Fabrication of metallic bipolar plate for proton exchange membrane fuel cells by rubber pad forming Author links open overlay panel, J. Power Sources 195 (11) (2010) 3529–3535.
46. Q. W, L. P, H.J.R. Jinbao Lin, Study on deformation behavior and strain homogeneity during cyclic extrusion and compression, J. Mater. Sci. 43 (2008) 6920–6924.
47. Q. W, J. L, L. Z, C.Z. Yongjun Chen, Fabrication of bulk ultra-fine grained magnesium alloys by cyclic extrusion compression, J. Mater. Sci. 42 (2007) 7601–7603.
48. B.R.S.N. Pardis, Cyclic expansion-extrusion (CEE): a modified counterpart of cyclic extrusion-compression (CEC), Mater. Sci. Eng. 528 (25–26) (2011) 7537–7540.
49. Yong Xue S.C.H.L., Effect of cyclic expansion-extrusion process on microstructure, deformation and dynamic recrystallization mechanisms, and texture evolution of AZ80 magnesium alloy, Adv. Mater. Sci. Eng.,vol 2019, 10 pages.

50. G.A.K.H. Alihosseini, Characterization of ultra-fine grained aluminum produced by accumulative back extrusion (ABE), Mater. Char. 68 (2012) 14–21.
51. N. Kamikaw, T. Furuhar, Accumulative channel-die compression bonding (ACCB): a new severe plastic deformation process to produce bulk nanostructured metals, J. Mater. Process. Technol. 213 (8) (2013) 1412–1418.
52. M. A. A. K. D. R. Moslem Tayyebi, Effects of strain accumulation and annealing on interfacial microstructure and grain structure (Mg and Al3Mg2 layers) of Al/Cu/Mg multilayered composite fabricated by ARB process, J. Manuf. Process. 22 (4) (2021).
53. F. Djavanroodi, B. Omranpour, M. Ebrahimi, M. Sedighi, Designing of ECAP parameters based on strain distribution uniformity, Progr. Nat. Sci.: Mater. 22 (5) (2012) 452–460
54. A. Azushima, R. Kopp, A. Korhonen, D.Y. Yang, F. Micari, G.D. Lahoti, P. Groche, J. Yanagimoto, N. Tsuji, A. Rosochowski, A. Yanagida, SeverePlasticDeformation (SPD)Processes for Metals, CIRP Ann. Manuf. Technol. 57 (2) (2008) 716–735.
55. Z.J. Zheng, Y. Gao, J.W. Liu, M. Zhu, A hybridrefining mechanism of microstructure of 304 stainlesssteel subjected to ECAP at 500 C, Mater. Sci. Eng. A. 639 (2015) 615–625.
56. I. Dimic, I. Chijovic-Alagic, B. Volker, A. Hohenwarter, R. Pippan, D. Veljovic, M. Rakin, B. Bugarski, Microstructure and metallic ion release of pure titanium and Ti–13Nb–13Zr alloy processed by high pressure torsion, Mater. Des. 91 (2016) 340–347.
57. Y.J. Chen, Y.C. Chai, H.J. Roven, S.S. Gireesh, Y.D. Yu, J. Hjelen, Microstructure and mechanical properties of Al-xMg alloys processed by room temperature ECAP, Mater. Sci. Eng. A 545 (2012) 139–147.
58. M.S. Shadabroo, A.R. Eivani, H.R. Jafarian, S.F. Razavi, J. Zhou, Optomization of interpass annealing for a minimum recrystallized grain size and further grain refinement towards nanostructured AA6063 during equal channel angular pressing, Mater. Characteriz. 112 (2016) 160–168.
59. V.L. Sordi, A.A. Mendes FilhoSordi, G.T. Valio, P. Springer, J.B. Rubert, M. Ferrante, Equal-channel angular pressing: Influence of die design on pressureforce, strain homogeneity, and corner gap formation, J. Mater. Sci. 51 (5) (2016) 2380–2393.
60. S.A. Nikulin, A.B. Rozhnopurv, S.O. Rogachev, V.M. Khatkevich, V.A. Turchenko, E.S. Khotulev, Investigation of structure, phase composition, and mechanical properties of Zr-2.5% Nb alloy after ECAP, Materials Letter. 169 (2016) 223–226.
61. M. Isik, M. Niinomi, K. Cho, M. Nakai, H. Liu, H. Yilmazer, Z. Horita, S. Sato, T. Narushima, Microstructural evolution and mechanical properties ofbiomedical Co–Cr–Mo alloy subjected to high-pressuretorsion, J. Mech. Behav. Biomed. 59 (2016) 226–235.
62. S.V. Dobatkina, O.V. Rybalchenko, N.A. Enikeev, A.J.S. Carpenter, T. Nizolek, R.J. McCabe, M. Knezevic, A. Tokar, M.M. Abramova, Formation of fully austenitic ultrafine-grained high strength state in metastable Cr–Ni–Ti stainless steel by severe plasticdeformation, Mater. Lett. 166 (2016) 276–279.
63. S.J. Zheng, B.P. Eftink, J.E. Scott, S.C. Vogel, T.M. Pollock, N.A. Mara, I.J. Beyerlein, Bulk texture evolution of nano lamellar Zr-Nb composites process via accumulative roll bonding, Acta Mater. 92 (2015) 97–108.
64. A. Fattah-alhosseini, S.O. Gashti, CorrosionBehavior of Ultra-fine Grained 1050 Aluminum Alloy Fabricated by ARB Process in a Buffer Borate Solution, J. Mater. Eng. Perform. 24 (9) (2015) 3386–3393.
65. S.S. Satheesh Kumar, T. Raghu, Strain path effects on microstructural evolution and mechanical behaviour of constrained groove pressed aluminium sheets, Mater. Des. 88 (2015) 799–809.
66. N. Haghdadi, A. Zarei-Hanzaki, H.R. Abedi, D. Abou-Ras, M. Kawasaki, A.P. Zhilyaev, Evolution of microstructure and mechanical properties in a hypoeutecticAl-Si-Mg alloy processed by accumulative back extrusion, Mater. Sci. Eng. A 651 (2016) 269–279.
67. G. Faraji, P. Yavari, S. Aghdamifar, M. Mosavi Mashhadi, Mechanical and microstructural properties of ultra-fine grained AZ91 magnesium alloy tube processed via multi pass tubular channel angular pressing(TCAP), J. Mater. Sci. Technol. 30 (2) (2014) 134–138.

68. Y. Estrin, A. Vinogradov, Extreme grain refinement by severe plastic deformation: A wealth ofchallengingscience, Acta Mater. 61 (3) (2013) 782–817.
69. D.H. Shin, J.J. Park, Y.S. Kim, K.T. Park, Constrained groove pressing and its application to grainrefinementofaluminium, Mater. Sci. Eng. A 328 (2002) 98–103.
70. F. Witte, The history of biodegradable magnesium implants: A review, Acta 6 (5) (2010) 1680–1692.
71. K. Inal, R.K. Mirshra, Crystal plasticity based numerical modelling of large strain deformation in hexagonal closed packed metals, Procedia IUTAM. 3 (2010) 239–273.
72. J. Levesque, K. Inal, K.W. Neale, R.K. Mishra, Numerical modelling of formability of extruded magnesium alloy tubes, Int. J. Plast 26 (2010) 65–83.
73. S.T. Adedokun, A review on equal channel angular extrusion as a deformation and grain refinement process, J. Emerg. Trends Eng. Appl. Sci. (JETEAS) 2(2) (2011) 360-363.
74. M. Kawasaki, T.G. Langdon, Review: Achieving superplastic properties in ultrafine-grained materials athigh temperatures, J. Mater. Sci. 51 (1) (2015) 19–32.
75. P.S. Roodposhti, N. Farahbakhsh, A. Sarkar, K.L. Murty, Microstructural approach to equal channel angular pressing of commercially pure titaniumA review, Trans. Nonferrous Met. Soc. China 25 (2015) 1353–1366.
76. Sabirov, M.Y. Murashkin, R.Z. Valiev, Nanostructured aluminium alloys produces by severe plastic deformation: New horizons in development, Mater. Sci. Eng. A 560 (2013) 1–24.
77. P.W.J. Mckenzie, R. Lapovok, ECAP with backpressure for optimum strength and ductility in aluminium alloy 6016.Part1:Microstructure, Acta Mater. 58 (2010) 3198–3211.
78. C.R. Ruiz, I.A. Figueroa, C. Braham, J.M. Cabrera, I. Alfonso, G. Gonzalez, Texture and lattice distortion sturdy of an Al-6061-T6 alloy produced byECAP, Mater. Trans. 56 (11) (2015) 1781–1786.
79. V.M. Segal, Equal channel angular extrusion: From macro mechanics to structure formation, Mater. Sci. Eng. A. 271 (1-2) (1999) 322–333.
80. Y. Huang, T.G. Langdon, Advance in ultrafine-grained material, Mater. Today 16 (3) (2013) 85–93.
81. Y. Iwahashi, Z. Horita, M. Nemoto, T.G. Langdon, The process of grain refinement in equal-channelangularpressing, Acta Metall. 46 (9) (1997) 3317–3331.
82. A. Bommareddy, M.Z. Quadir, M. Ferry, Time and temperature regime of continuous grain coarsening in an ECAP-processed Al (0.1wt%Sc) alloy, J. Alloy. Compd. 527 (2012) 145–151.
83. M. Avvari, S. Narendranath, Influence of route-R on wrought magnesium AZ61 alloy mechanical properties through equal channel angular pressing, J. Magn. Alloy. 2 (2) (2014) 159–164.
84. J. Suh, J. Victoria- Hernandez, D. Letzig, R. Golle, S. Yi, J. Bohlen, W. Volk, Improvement in cold formability of AZ31 magnesium alloy sheets processed by equal channel angular pressing, J. Mater. Process. Technol. 217 (2015) 286–294.
85. F. Dalla Torre, R. Lapovok, J. Sandlin, P.F. Thomson, C.H.J. Davies, E.V. Pereloma, Microstructuresand properties of copper processed by equal channel angular extrusion for 1–16 passes, Acta Mater. 52 (16) (2004) 4819–4832.
86. W. Blum, J. Dvorak, P. Krai, P. Eisenlohr, V. Sklenicka, Effect of grain refinement by ECAP on creep of pure Cu, Mater. Sci. Eng. A 590 (2014) 423–432.
87. H.S. Kim, W.Y. Kim, K.H. Song, Effect of post-heat-treatment in ECAPprocessedCu-40%Znbrass, J. Alloy. Compd. 536 (2012) 200–203.
88. Y. Fukuda, K. Oh-ishi, Z. Horita, T.G. Langdon, Processing of a lowcarbonsteelbyequal-channelangularpressing, Acta Mater. 50 (6) (2002) 1359–1368.
89. K.R. Cardospo, D.N. Travessa, W.J. Botta, A.M. Jorge Jr., High strength AA7050 Al alloy processed by ECAP: Micro structurend mechanical properties, Mater. Sci. Eng. A 528 (2011) 5804–5811.

